63-3-5

405571

405 571

TI REPORT NUMBER
08-63-63

QUARTERLY PROGRESS REPORT

for

MOLTEN-CARBONATE FUEL BATTERY PROGRAM

Contract No. DA-44-009-AMC-54(T)

U.S. Army Engineer Research &
Development Laboratory

This Report Covers the Period 15 February 1963
through 15 May 1963

TEXAS INSTRUMENTS INCORPORATED

DDC

JUL 3 1963

USIA B

TI REPORT NUMBER
08-63-63

QUARTERLY PROGRESS REPORT

for

MOLTEN-CARBONATE FUEL BATTERY PROGRAM

This Report Covers the Period 15 February 1963 through 15 May 1963

Texas Instruments Incorporated
13500 North Central Expressway
Dallas 22, Texas

Contract No. DA-44-009-AMC-54(T)

U. S. Army Engineer Research & Development Laboratory

QUARTERLY PROGRESS REPORT

for

MOLTEN-CARBONATE FUEL BATTERY PROGRAM

Contract No. DA-44-009-AMC-54(T)

TABLE OF CONTENTS

TABLE OF CONTENTS
(Continued)

LIST OF FIGURES

TABLE OF CONTENTS
(Continued)

LIST OF FIGURES
(Continued)

QUARTERLY PROGRESS REPORT
FOR
MOLTEN-CARBONATE FUEL BATTERY PROGRAM

Contract No. DA-44-009-AMC-54(T)

SUMMARY

Power obtainable from single cells on hydrogen fuel using the 4 3/16 in. electrode diameter assembly has been increased from an average of 60 watts to about 100 watts per square foot at 0.7 volts by improvements in the fuel electrode structure and reduction in electrical resistance. These cells produce approximately 60 watts per square foot at 0.5 volts on a fuel composed of 50:50 hydrogen and carbon dioxide. Cells have operated on the 50:50 hydrogen-carbon dioxide mixture for more than 1,000 hrs. A concentration of 0.2 mole percent of hydrogen sulfide in the fuel gas was not found detrimental in a 1,000 hr test. A 100-watt battery design has been constructed. We are continuing to work out difficulties encountered with shorting and leaks.

A laboratory model of the JP-4 - air partial oxidation unit has produced 12.5 cu ft/hr of a gas stream containing 50-60 percent gaseous fuel (mostly hydrogen and carbon monoxide), 35-40 percent nitrogen, and 5-10 percent carbon dioxide. This unit has been operated for 78 continuous hours. A cell has been operated directly on the gaseous product. A larger unit with a design output of 70 cu ft/hr is being constructed.

A series of five additives for the molten-carbonate electrolyte has been screened, (Na_2MoO_4, Na_2CrO_4, Na_2WO_4, Na_2S, and Na_2ZnO_2). Only sodium sulfide was observed to have a significant positive effect on cell power output. Preliminary investigation of the coulostat method of active area determination

has indicated that the method is unsuitable for the molten-carbonate fuel cell system. Polarization and current interrupter studies of anodes fueled with simulated reformed hydrocarbons indicate no adverse anode polarization over results obtained using hydrogen fuel.

J. K. TRUITT, Project Manager
Energy Research Laboratory

C. G. PEATTIE, Director
Energy Research Laboratory

QUARTERLY PROGRESS REPORT

for

MOLTEN-CARBONATE FUEL BATTERY PROGRAM

Contract No. DA-44-009-AMC-54(T)

I. OBJECTIVE

The purpose of this program is to continue the development of the molten-carbonate fuel cell into a practical electric power source operated on liquid hydrocarbon fuels.

Task I

Research and development of a high temperature molten-carbonate saturated hydrocarbon air fuel cell by investigating electrolyte-electrode interface resistances, electrode forming techniques, and unit cell operating problems, and by assembling a battery of cells to produce 100 watts of electric power.

1. Study Causes of Cell Resistances

(a) Determine active surface areas of various electrodes by Dr. Paul Delahay's "Coulostat Method for Kinetics Study of Fast Electrode Processes" and other available techniques.

(b) Study effects of (1) particle size of starting materials; (2) pressing pressure, time and temperature; (3) sintering time, temperature, and atmosphere; and (4) binders, burnout, and other leachable additives on electrode performance.

(c) Study effects of varying electrode and electrolyte composition on the cell performance.

2. Electrode Fabrication

Fabricate cylindrical, flat plate, and horizontal bed electrodes and test mechanical and electrochemical performances.

3. Battery Assembly

(a) Assemble unit cells to produce 100-watt batteries and test their mechanical and electrochemical characteristics.

(b) Study effects of quick start-up times and cycling of cells (from 30°F to operating temperature) on cell performance and life.

(c) Deliver one of the batteries of the unit cells in the form of a portable 100-watt battery system that will have its own self-contained heater, fuel supply, and carbon dioxide recirculating mechanism.

II. TASK I - STUDY CAUSES OF CELL RESISTANCE

By Isaac Trachtenberg, K. W. Kreiselmaier, J. F. Haefling

A. Task I-1

1. Introduction

The fuel cell under investigation contains two working electrodes (anode and cathode) bonded to a 3 3/16 in. diameter magnesium oxide (MgO) disc. The MgO disc is impregnated with a binary eutectic of $LiNaCO_3$ (m.p. ca. 500°C). Some typical operating data for a complete fuel cell of the type described are shown in Fig. 1. Considerable information concerning the complete cell can be obtained from these data. However, to establish the causes of cell resistance (polarization) it is necessary to study the individual anodes and cathodes of the working cell.

Figure 2 is an illustration of the cathode chamber of the cell with the third idling electrode. This electrode is used to monitor the performance of the individual anode and cathode in the working fuel cell. The small electrode, 0.5 cm^2, is a reference or non-working electrode. The large one (15.6 cm^2 or 1/60 ft^2) is the working cathode. Not shown is the anode on the bottom side of the MgO disc. The anode has the same geometric configuration as the working cathode. The MgO disc is impregnated with the binary $LiNaCO_3$ eutectic. Electrical connections are made from the electrodes to the various insulated lead-throughs. The only electrical connection within the cell between the three electrodes is through the electrolyte contained in the porous MgO disc. The lids are welded on to make each chamber gas tight, the cell is placed vertically in a furnace, and the necessary external gas and electrical connections are completed.

Current-voltage traces for the complete working cell and the individual electrodes were obtained with a Moseley Model 3S X-Y recorder. A transistor network, Fig. 3, is used to give a continuously variable, pure resistive load for the cell. The current passed in this circuit is the X-input.

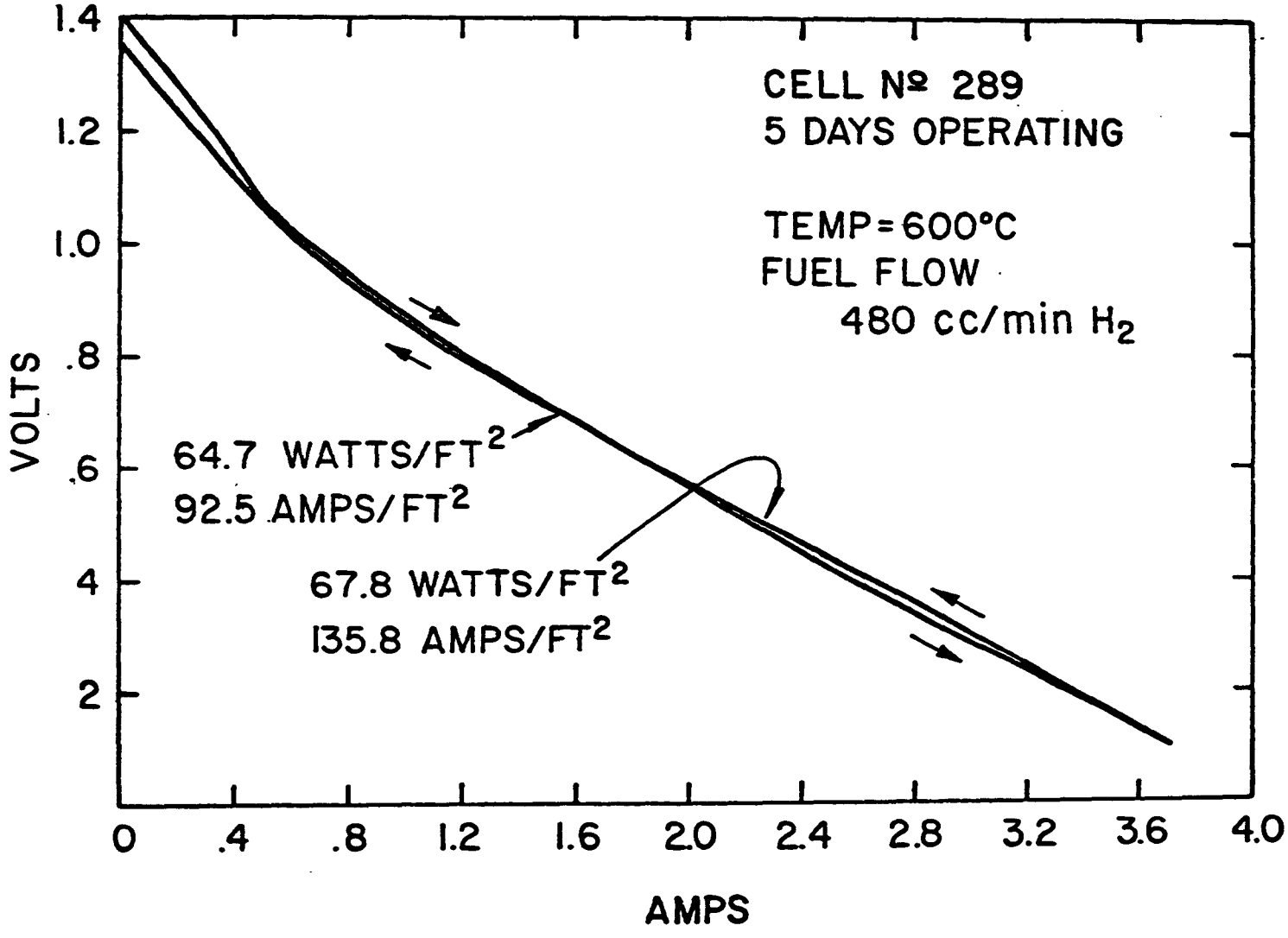

Fig. 1 Characteristic Performance Curve

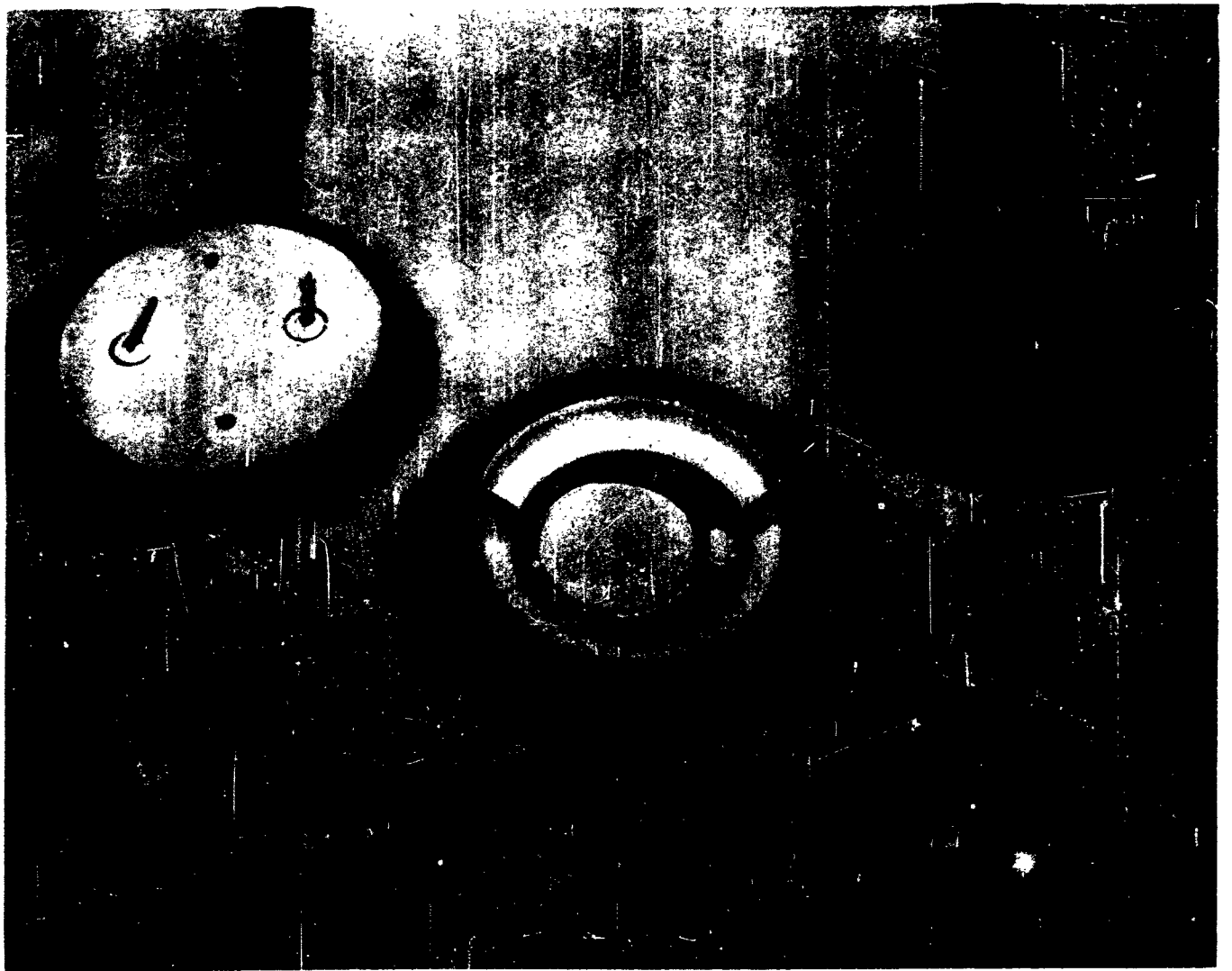

Fig. 2 Reliability Cell Components

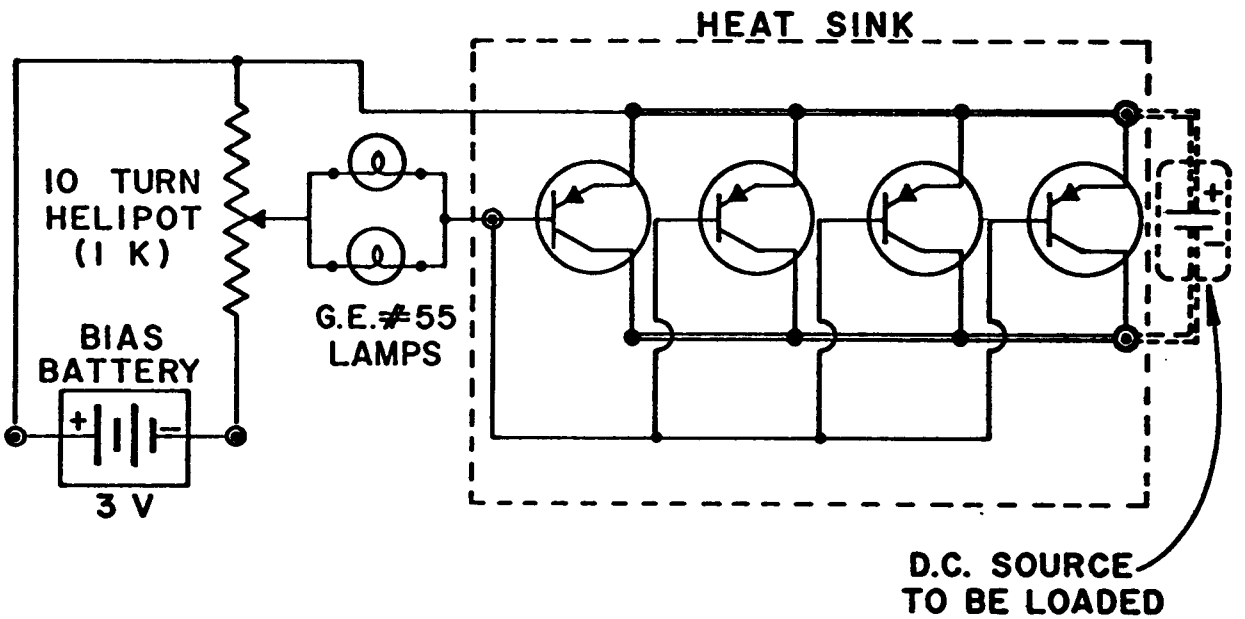

Fig. 3 Transistorized Variable DC Load Bank

The voltage between the non-working electrode and the particular working electrode to be studie (the terminal voltage of the cell) becomes the Y-input. To avoid polarization of the non-working electrode, the Y-input (or for that matter, any voltage measuring device used with the non-working electrode) must have a high input impedance. These current-voltage curves measure the total steady state polarization of the individual electrodes and the complete cell under working conditions.

2. Current-Voltage Curves for Operating Cell

The specific results presented are typical examples of the data obtained from a large number of experiments on many similar cells. Figure 4 shows current-voltage curves for a cell operating at 600°C on pure H_2 fuel on the 25th day of operation. The cathode is supplied with a 4:1 mixture of air:CO_2. The curve V_T represents the terminal voltage of the operating cell. The open circuit voltage is 1.40 volts. V_A and V_C curves are the voltage of the anode and cathode, respectively, vs the non-working electrode. The values of R_A and R_C, the ohmic resistances as determined by current interruption, were measured at several pre-interruption currents and found to be constant. Correction for the ohmic polarization is made, and the curves $V_A + IR_A$ and $V_C - IR_C$ are the current-voltage curves resulting from concentration polarization. It is interesting to note that $R_A + R_C < R_T$. This difference is assumed to be the bulk electrolyte resistance, R_E. In addition to the ohmic resistance at the electrode-electrolyte-matrix interface, R_A and R_C contain the resistance of the individual electrode leads to the terminals just outside the furnace. For the particular case of cell 117R at 600°C, R_A, R_C, and R_T are 0.075, 0.10, and 0.21 ohms, respectively; the lead resistance of the individual electrodes is about 0.025 ohms. R_E is calculated to be 0.035 ohms. The calculated resistance based on electrolyte conductivity, electrode size, and separation is 0.011 ohms. These calculations imply a factor of about 3 due to porosity and tortuosity of the MgO disc.

The V_T curve indicates a power density equivalent to 60 W/ft^2 at 0.7 volts. If all ohmic factors except the bulk electrolyte resistance, R_E,

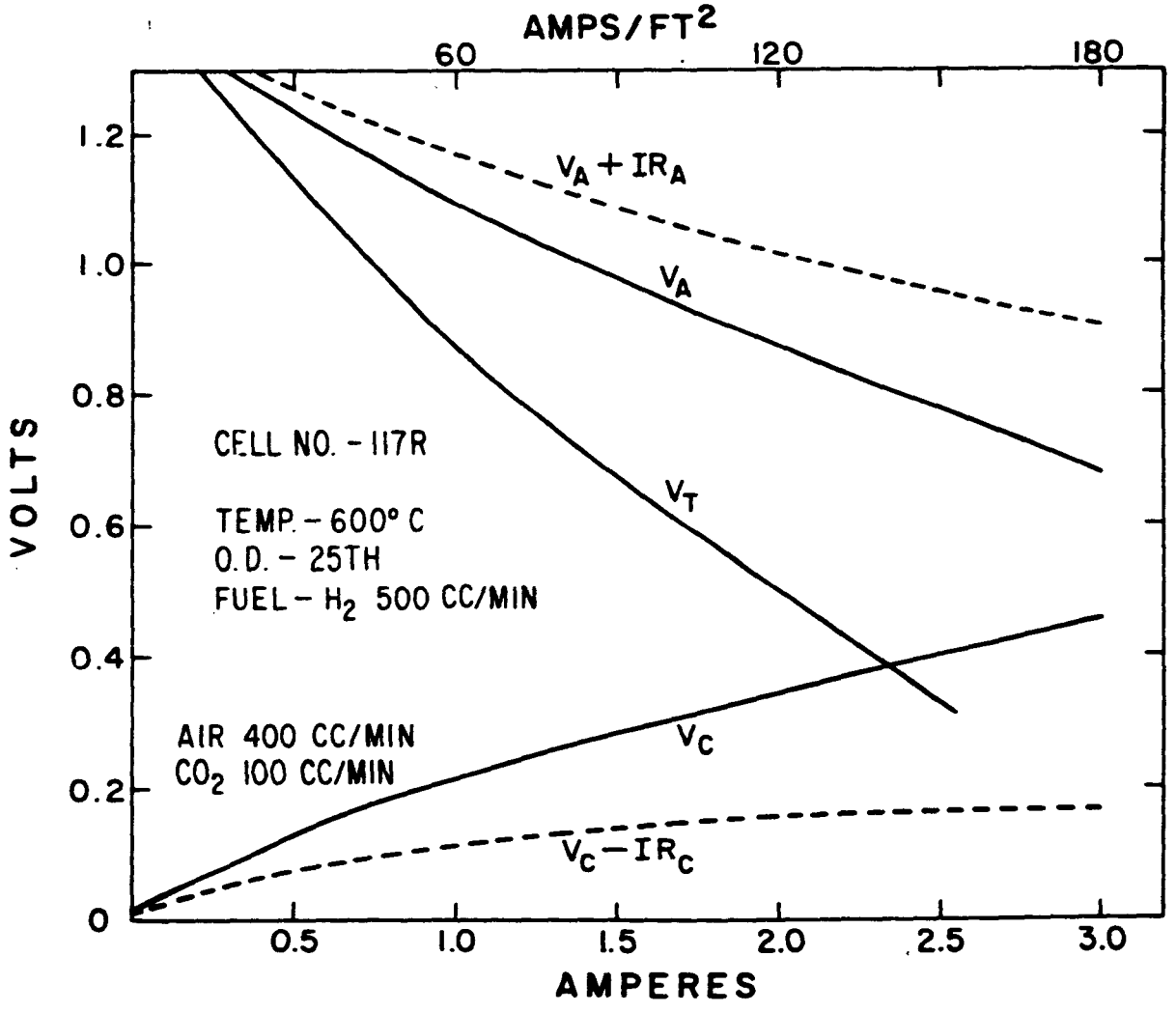

Fig. 4 Electrode Polarization Characteristics with Hydrogen

could be removed, this cell would produce an equivalent of 120 watts/ft^2 at 0.7 volts.

Several features concerning the polarization of the individual electrodes should be pointed out. Limiting currents are not being approached, even at current densities of 200 amps/ft^2. Ohmic polarization is a more important factor at the cathode, where oxide films may be formed. Concentration polarization is greater at the anode, since products must back-diffuse.

Figure 5 shows additional current-voltage curves for cell 117R. To obtain these data, 200 cc/min of CO_2 were added to the original H_2 fuel supply. This fuel represents a reformed hydrocarbon. The cathode conditions were unchanged, and the polarization curves obtained were the same as in Fig. 4. The effect of additional flow rate only is negligible (H_2 rate was raised to 700 cc/min with no measurable change in the current-voltage curve). The effect of adding CO_2 was observed immediately, even at open circuit. Considerable amounts of water were obtained in the fuel effluent. The values of R_A, R_C and R_T were not altered by the change in fuel composition. However, the open circuit voltage is markedly reduced; this effect can be attributed to the introduction of CO_2 and the formation of H_2O from the water-gas shift equilibrium. These substances are products from the over-all anode process.

The terminal power output is equivalent to 42 watts/ft^2 at 0.7 volts, and if all ohmic factors but bulk electrolyte resistance were eliminated, an equivalent power of about 84 watts/ft^2 at 0.7 volts could be obtained. It should be noted in comparing Figs. 4 and 5 that the concentration polarization, 0.18 volts, at an equivalent of 100 amps/ft^2 for reformed hydrocarbon fuel is considerably lower than that of the pure H_2 fuel, 0.35 volts, at the same current density. However, the open circuit voltage and the operating voltage are lower for the reformed fuel, 1.06 volts open circuit compared to 1.40 volts open circuit for the pure H_2 fuel.

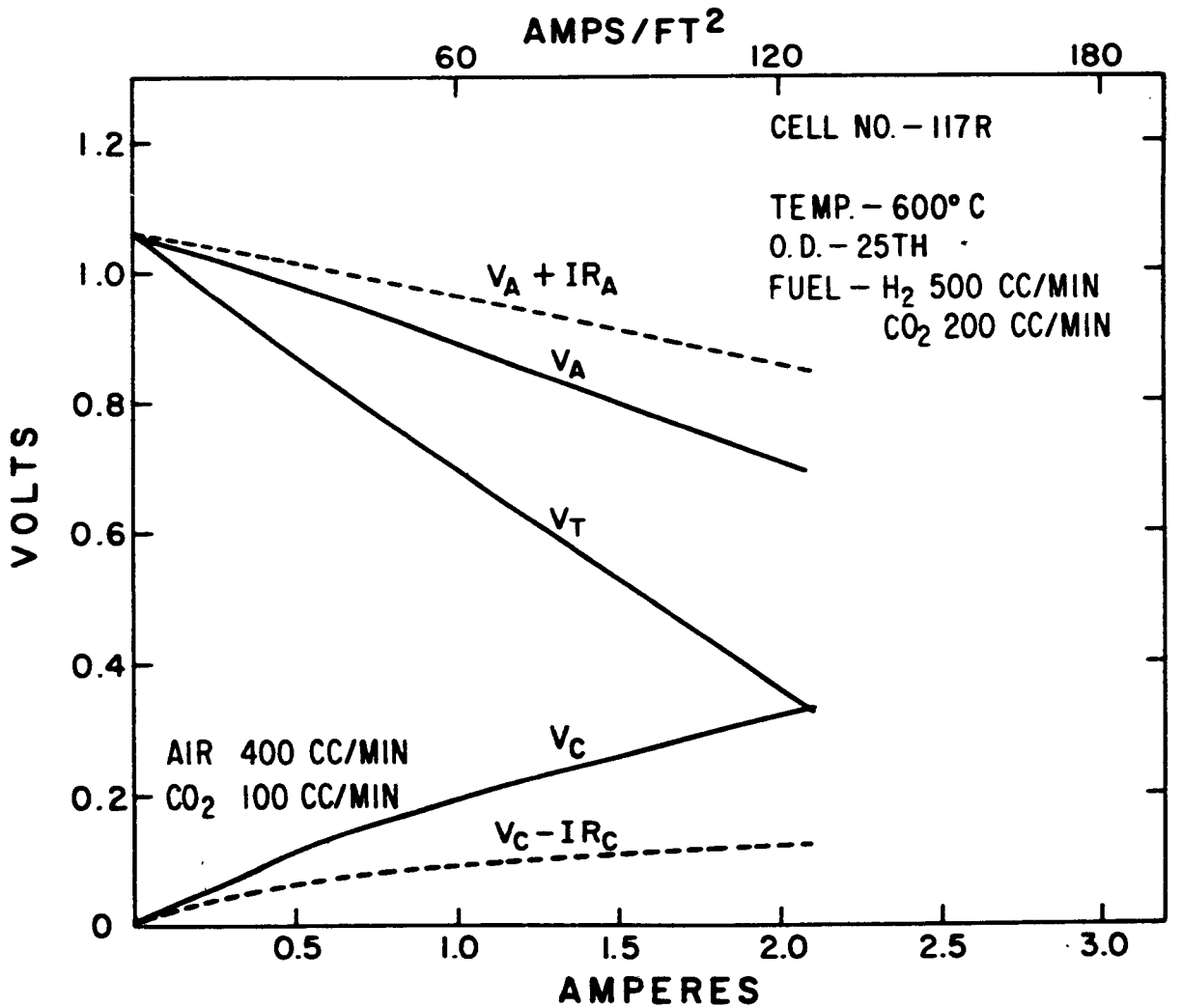

Fig. 5 Electrode Polarization Characteristics with Hydrogen and Carbon Dioxide

What has been referred to as concentration polarization until now is really total polarization minus ohmic polarization. From data such as these and current interruption studies, no activation polarization or evidence of any could be detected. As might be expected, the system is subject to less concentration polarization as product concentration of the incoming fuel increases.

3. Current Interruption Studies

A transient method is necessary to establish the contributions of the various types of polarization (ohmic, activation, and concentration) to the total polarization. A single current interruption technique was used for this purpose. The three types of polarization of interest may be distinguished according to time intervals after removing the polarizing load. Ohmic polarization is removed after current interruption for the present investigation in times less than a microsecond. Since removing activation polarization requires the electrode potential to change, the time required for its decay is governed by the rate of charging of the electrical double layer, or about 10^{-6} to 10^{-4} seconds. Polarization decay caused by concentration effects requires times greater than 10^{-4} seconds, because appreciable mass transport (either ions in the electrolyte or molecules in the gas phase) must occur.

Figure 6 schematically shows the interruption circuit. The heart of this circuit is the mercury-wetted Clare relay and its make-before-break operating feature. This feature permits triggering and use of the sweep delay circuits of the 545A oscilloscope. Typical operating sequence is as follows: the desired load is selected and the relay energized (normally open contacts closed). The cell is allowed to come to equilibrium; usually a few seconds to several minutes are required. The relay is de-energized. The normally closed contact is made 1 millisecond before the normal open contact opens; a signal is obtained from the normally closed contacts and serves as triggering input to a Tektronix 545A oscilloscope. The scope is set up so that the actual sweep may be delayed from a few microseconds up to several milliseconds. This arrangement is used to obtain time scale on voltage-time records

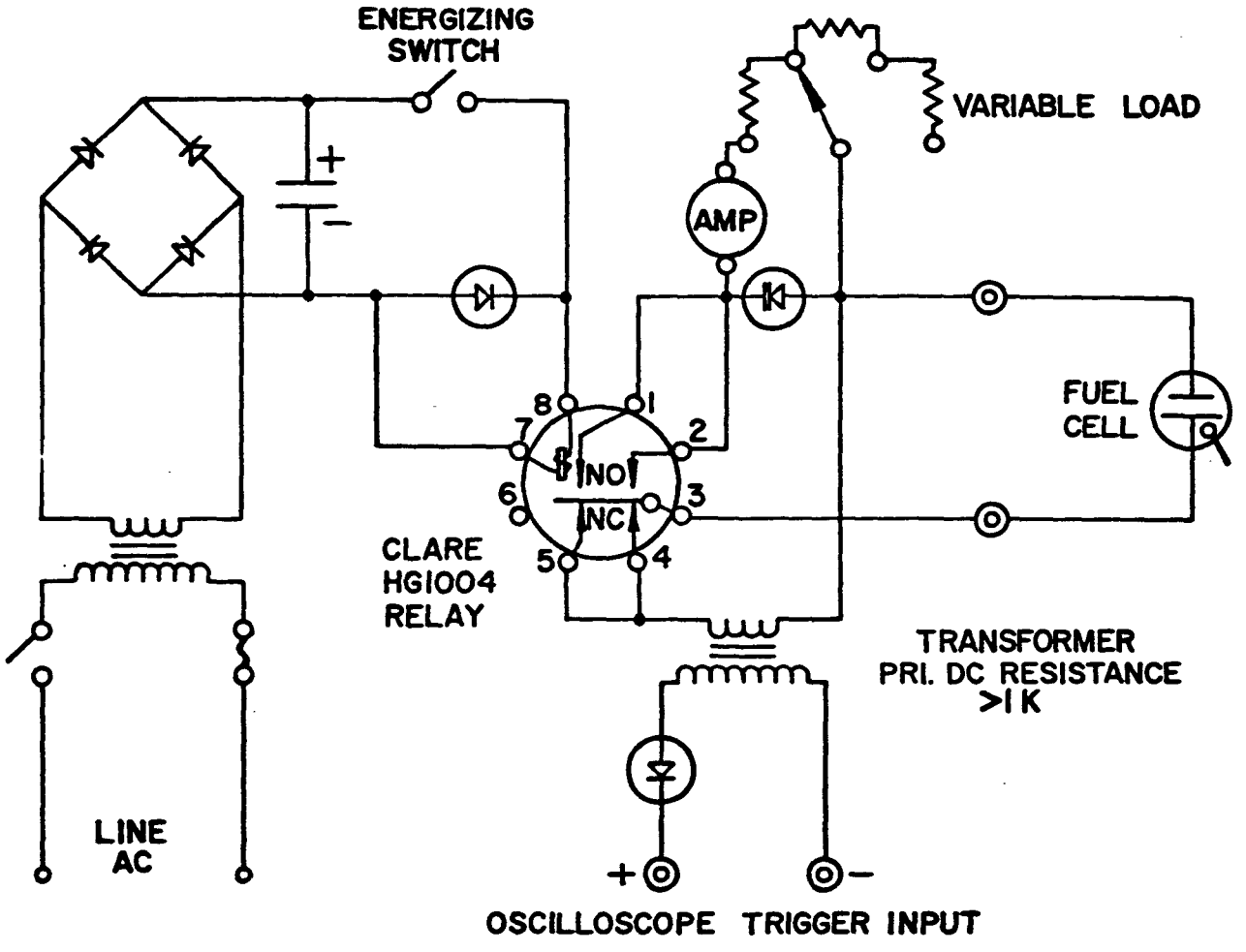

Circuit used to obtain voltage–time curve < 1 sec.

Fig. 6 Interrupter Circuit

from 5×10^{-7} to 1×10^{-3} seconds/cm. When the time scale is longer than 1×10^{-3} seconds, no sweep delay is required. In all instances the voltage recorded is that of a working electrode vs the non-working electrode.

As we have mentioned, ohmic, activation, and concentration polarization may be distinguished and measured by voltage decay as a function of time after interruption of a steady state current. A previous publication[1] was concerned only with pure H_2 fuel in this system. Hydrogen is compared here with simulated reformed hydrocarbon fuels.

Figure 7 illustrates anode current-voltage curves corrected for ohmic polarization. Open circuit voltage decreases with decreasing flow rate and increasing product (CO_2 and H_2O) concentration. However, polarization at any given current density decreases with increasing product concentration of the incoming fuel. The lower open circuit voltage of curve B compared to curve A is related to the amount of CO_2 continuously escaping from the electrolyte and the relative concentration of CO_2, H_2O and H_2.

Current interruption experiments were completed with the fuels indicated in Fig. 7. All measurements were made at a pre-interruption current equivalent to a current density of 60 amps/ft^2. Figure 8 illustrates the voltage-time curves for the two high fuel flow rates. The two straight lines are characteristic of this type of measurement. The steady state polarization is represented by the symbols through the ordinate. The initial drop is the same for all fuels and flows studied. Data in the 10^{-6} range are somewhat distorted by the ring-back voltage which develops when the current drops instantly to zero. The horizontal line in the 10^{-5} to 10^{-4} second range indicates no measurable activation polarization. The polarization decay in times greater than 10^{-4} are attributed to concentration effects. The two curves are almost parallel. At the high flow rates used, any effect of flow rate has been removed. Since polarization for the H_2-CO_2 fuel is less than that for pure H_2, the H_2-CO_2 open circuit voltage is attained more rapidly.

---

1. I. Trachtenberg, J. Electrochem. Soc. (in press) 1963.

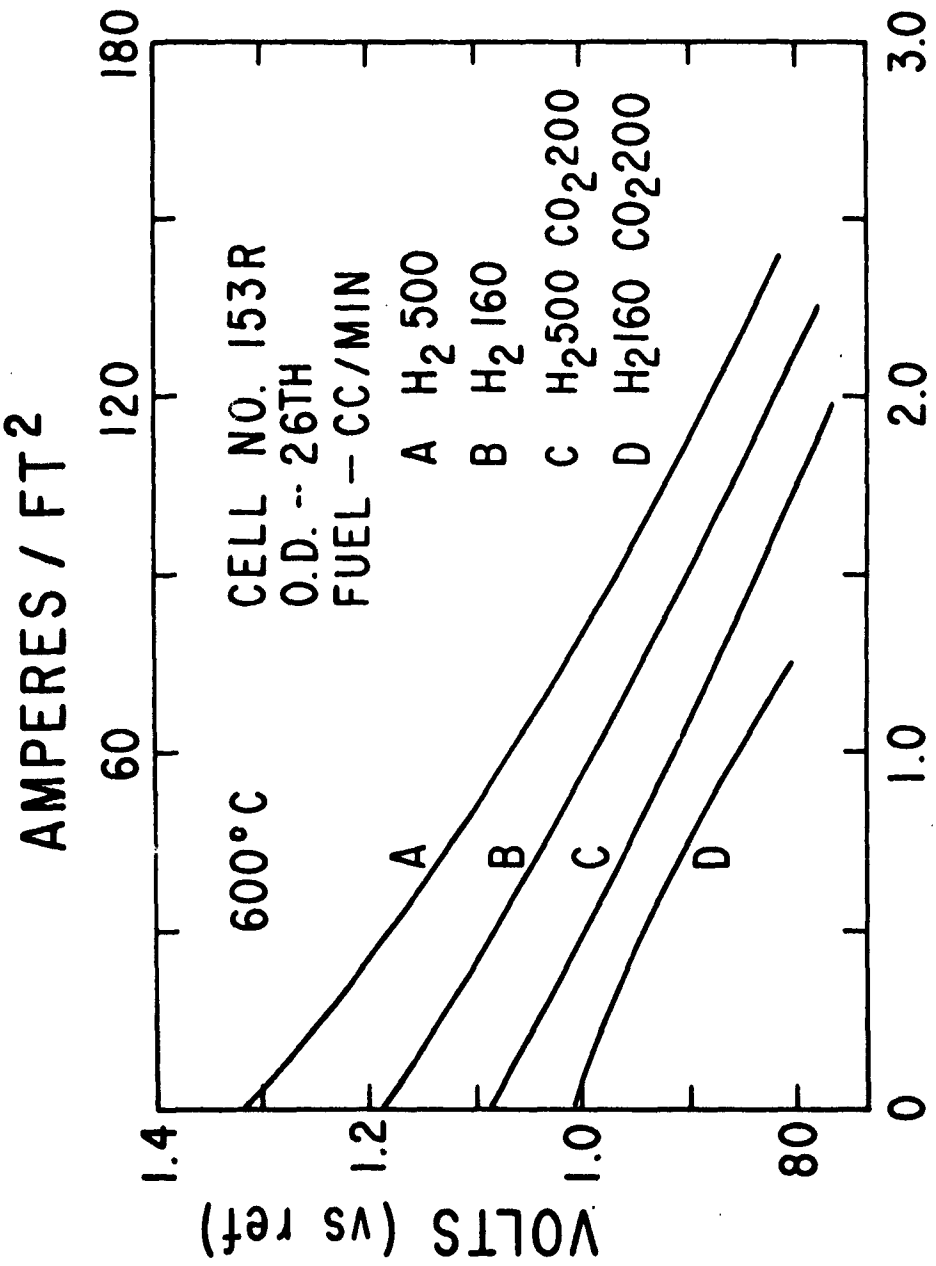

Fig. 7 Voltage Characteristics with Various Fuels

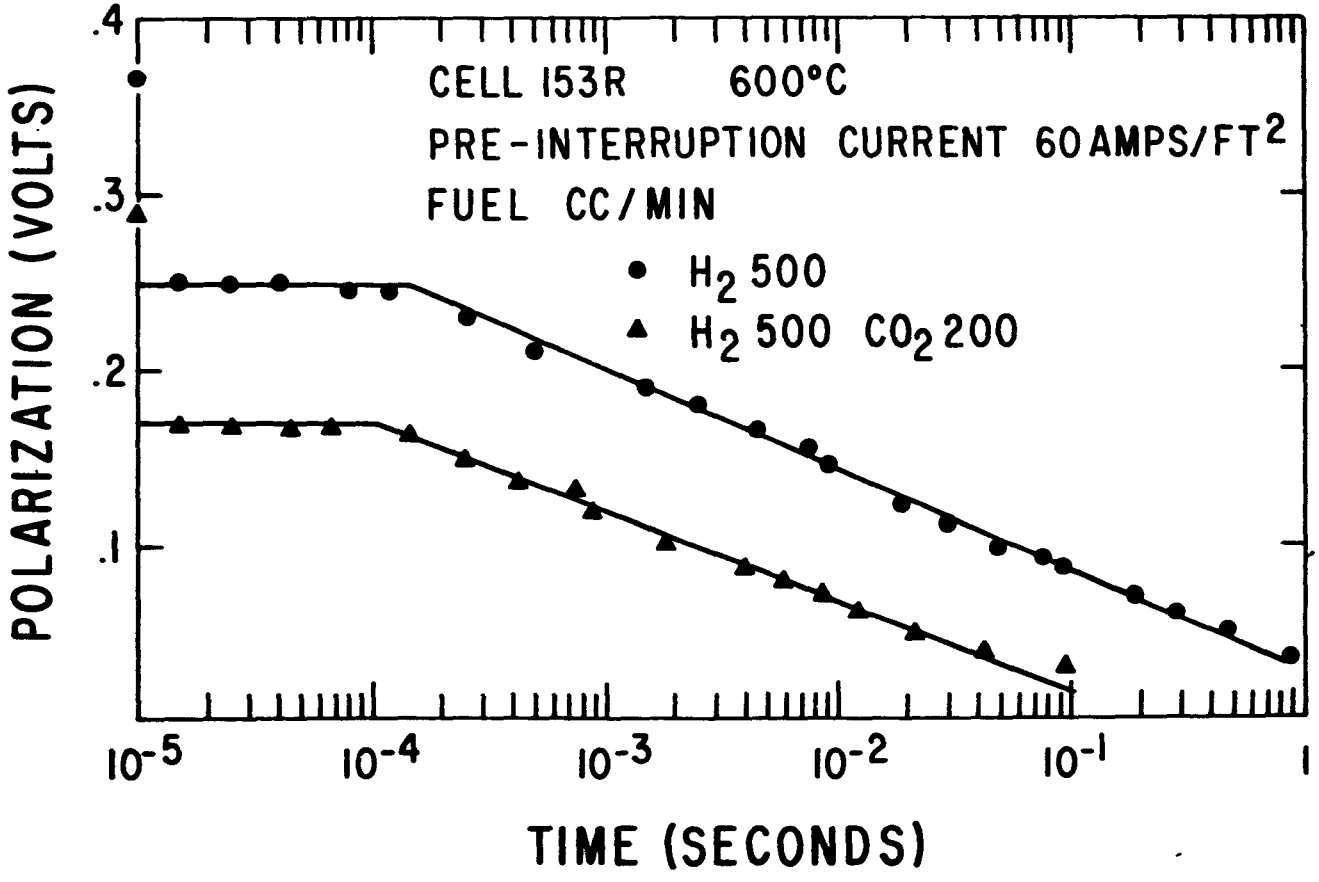

Fig. 8 Interrupter Polarization Characteristics of Anode at High Flow Rates

Figure 9 illustrates the voltage-time curves for the lower flow rates of Fig. 7. The same characteristic features are observed here as in Fig. 8. The ohmic polarization is constant, and there is no measurable activation polarization. However, there is an effect of flow rate. The total flow of 360 cc/min for the H_2-CO_2 case increases the decay rate of concentration polarization over that observed for pure H_2 at 160 cc/min.

The effect of flow rate on anode polarization curves was studied in another series of experiments. In Fig. 10 anode polarization curves corrected for ohmic polarization at various fuels and flow rates are presented. Curve I illustrates that cells operating on reformed hydrocarbons at high flow rates perform better than on pure H_2, even though the open circuit voltage is higher for the pure fuel. Introducing an inert gas to aid sweep (curve III) leads to high open circuit voltage but much more rapid polarization (compare curves II and III) when placed under load.

All data relating to flow rates indicate that the benefits of high open circuit voltage obtained by high flows of pure hydrogen or hydrogen diluted with inert gases are lost when significant quantities of the fuel are consumed. The effect of the high flow rates of gases is to reduce the concentration of non-electrochemically produced CO_2 and H_2O. When the electrochemical processes are functioning, this effectiveness of gas sweeping is greatly reduced.

Interruption studies were made on cathodes. Figure 11 is a typical voltage-time plot for a cathode operating on a 4:1 mixture of air:CO_2. The curves are very similar to those obtained for anodes. Cathodes exhibit higher ohmic polarization than anodes and less concentration polarization. Cathodes are not as sensitive to gas flows. Since concentration polarization is small, electrode steady state is rapidly attained.

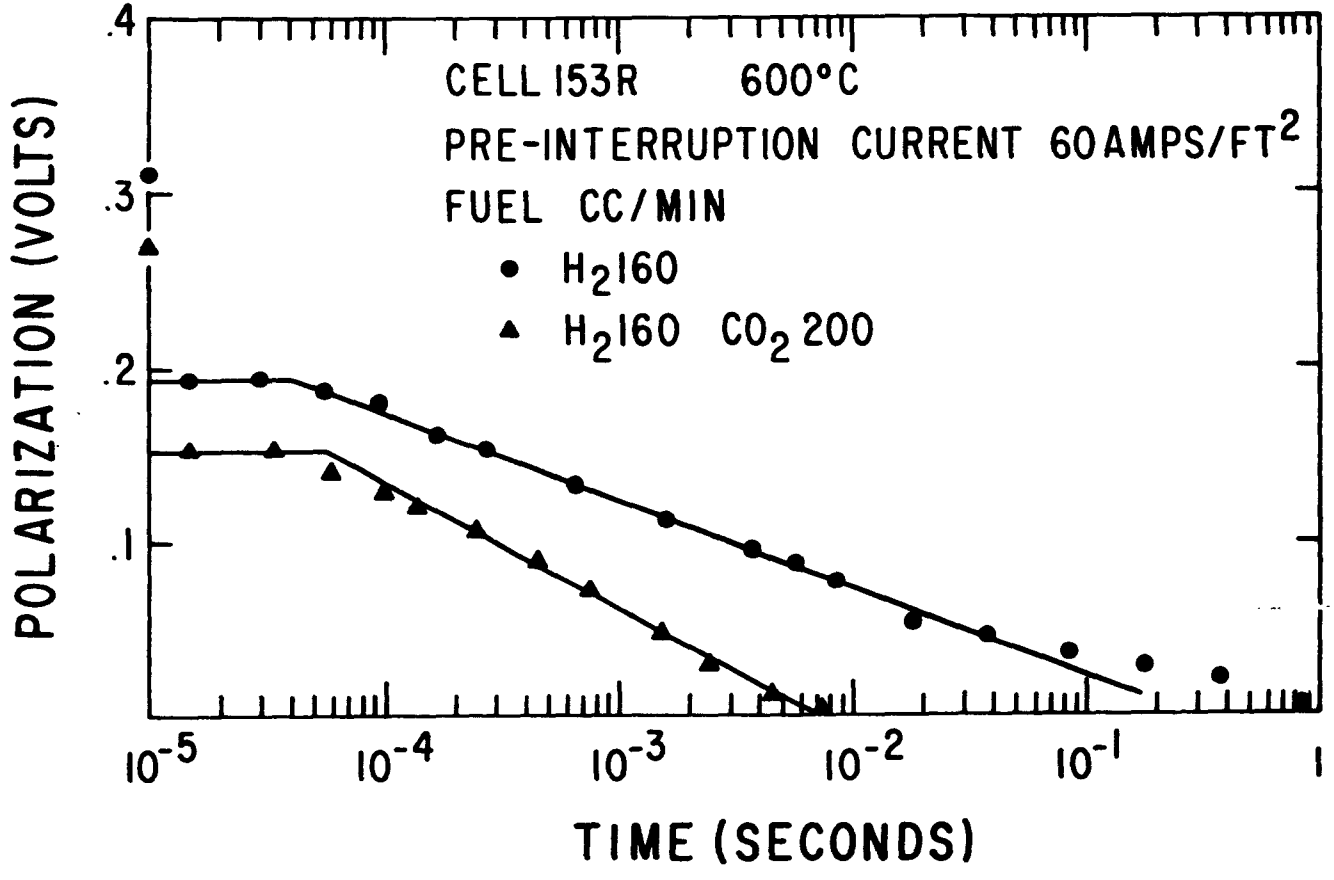

Fig. 9 Interrupter Polarization Characteristics of Anode at Low Flow Rates

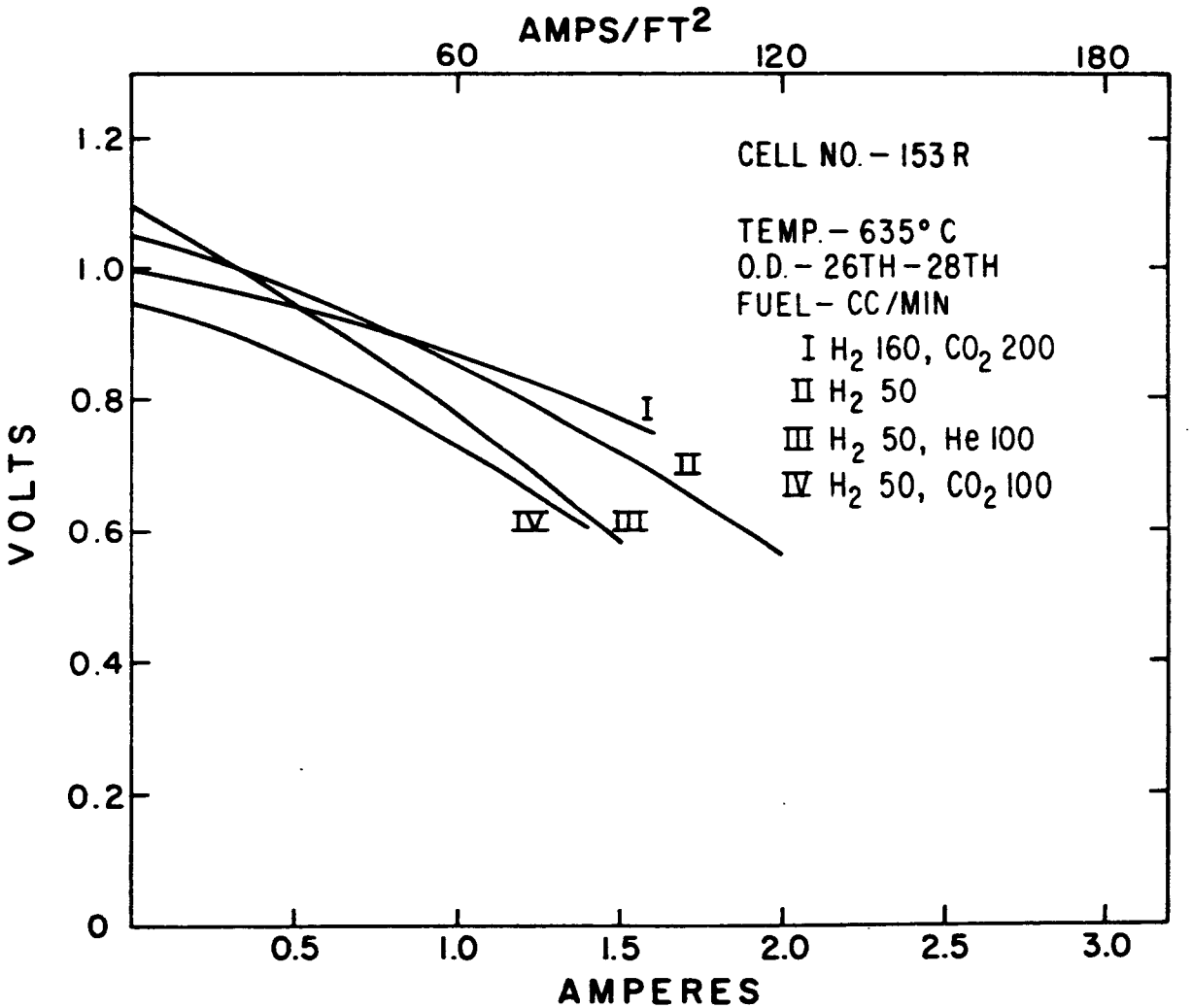

Fig. 10 Anode Polarization with Various Fuel Compositions

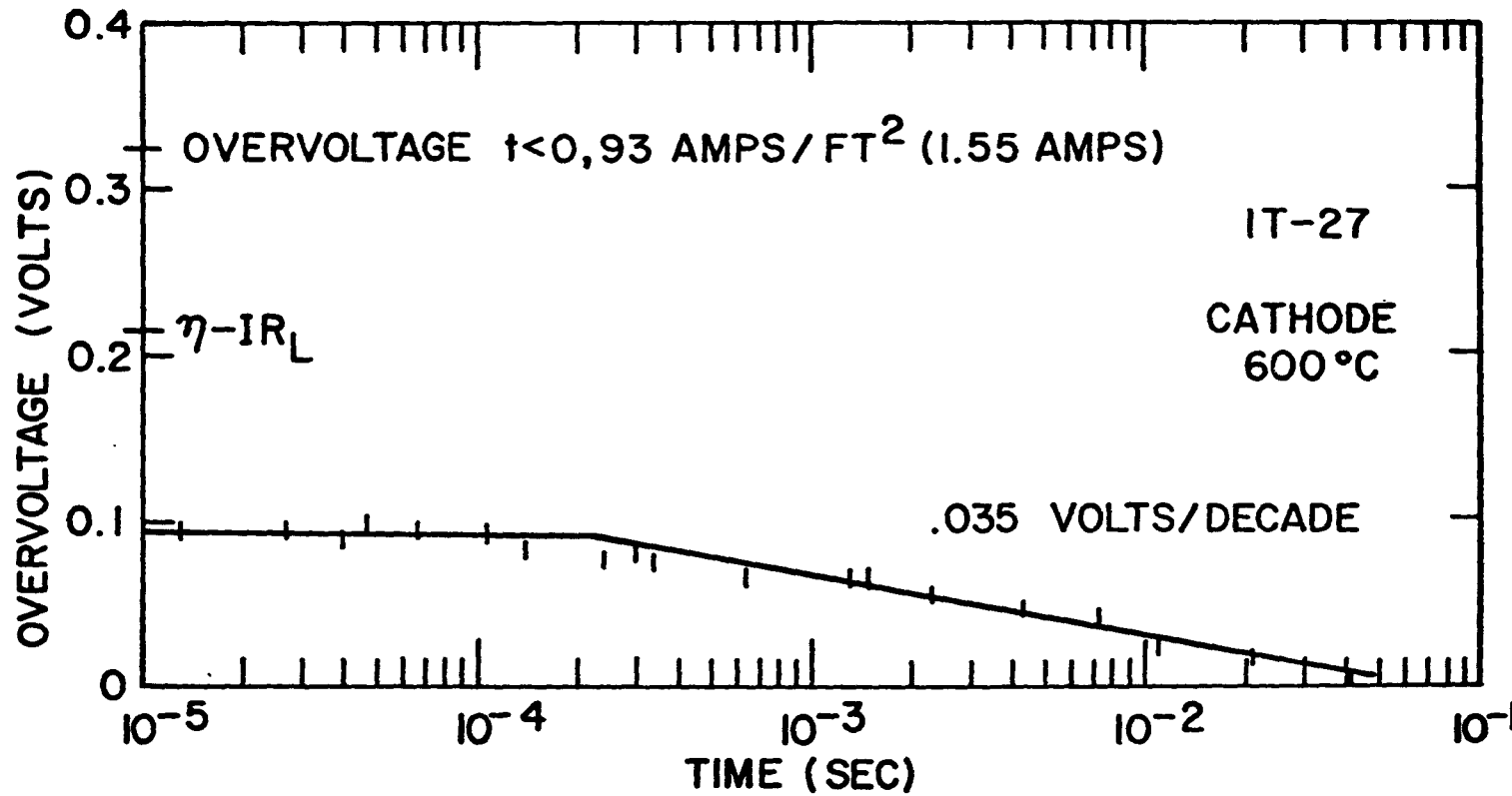

Fig. 11 Interrupter Polarization Characteristics of Cathode

4. Ohmic Polarization and Electrolyte Resistance

Ohmic resistance at the individual electrodes is calculated from the initial (10^{-6} second) voltage decay and the pre-interruption current. The values determined include lead resistance (0.025 ohms). Bulk electrolyte resistance is determined by subtracting the sum of the anode and cathode resistance from the total cell resistance.

The temperature coefficients of the various resistances were measured. The anode coefficient was nearly identical to that of the bulk electrolyte, while the coefficient of the cathode was much higher (resistance decreased more than would be predicted on the basis of changes in electrolyte conductivity alone).

The relatively high ohmic polarization at the anode, the consequence of ohmic resistance, may be attributed to electrolyte restriction at the electrode-matrix interface. It is very unlikely that all pores of the electrode match the pores in the matrix. In fact, there is a great deal of masking. This masking greatly reduces the thickness and number of electrolyte paths between the active electrode sites and the bulk electrolyte and increases the ohmic resistance. Since the temperature coefficient of the ohmic resistance at the anode is the same as that of the bulk electrolyte, it is reasonable to assume that all the ohmic polarization at this electrode results from the electrolyte. Its relatively large value is directly attributable to the degree of electrolyte restriction.

At the cathode a similar situation exists. However, there is an additional contribution to the ohmic resistance which has a larger temperature coefficient. Although silver oxide is thermally unstable at 600°C, there is a finite amount present on the electrodes. This oxide layer introduces some additional ohmic resistance. As the temperature is increased, the amount of oxide is reduced and the ohmic polarization decreases.

5. Conclusion

Fuel cells employing molten-carbonate electrolytes can be operated successfully on air and a wide variety of fuels readily derived from hydrocarbons. At current densities up to 200 amps/ft^2 there is no kinetic limitation other than mass transport.

When hydrocarbon-derived fuels are initially supplied to the anode, open circuit voltage is lower than when pure H_2 is supplied. However, under appreciable load, anode polarization on impure fuel is much lower. Cathodes perform well on mixtures of air and CO_2.

Total cell polarization can be accounted for as the basis of ohmic and concentration polarization. There is no evidence of activation polarization on any of the electrodes investigated. Catalysts may affect the over-all performance of the cell by establishing the H_2O-H_2 adsorption equilibrium. This may vary for different catalysts. However, it is a thermodynamic effect of the system and not a result of kinetic limitation.

B. Task I-1a. Determine Active Surface Area

An attempt was made to determine the active surface area for various electrodes by using a method suggested by Dr. Paul Delahay in "Coulostat Method for the Kinetics Study of Fast Electrode Processes."[2] This method is based on the fact that if additional charge is rapidly placed on the electrode, the potential of the electrode must change. The rapid discharge of a capacitor is used to supply the additional charge to the electrode. The change in potential is followed on an oscilloscope. These data permit calculation of the double layer capacity of a given electrode. By previously calibrating to establish the double layer capacity per unit area, it is possible to determine the electrochemically active surface area.

---

2. P. Delahay, J. Phys. Chem. 66, 2204-2208 (1962).

Since this method depends on displacement from an equilibrium position, the initial equilibrium must be very steady and reproducible. This implies a steady state potential for the electrode with a maximum variation of ± 2 millivolts, and preferably ± 1 millivolt. An additional requirement of the electrochemical system is that the capacitive impedance should be less than the resistive impedance.

The molten-carbonate fuel cell under investigation now fails to meet both of these requirements. CO_2 constantly escapes from the electrolyte, resulting in constantly changing fuel composition at the electrode-electrolyte interface. This produces a continuously varying electrode potential. Potential measurements must be made in times less than 10^{-4} seconds, preferably less than 10^{-5} seconds. The variation of electrode potential due to fuel composition changes is non-periodic in this short time interval. The rather lower resistance exhibited by molten carbonates, coupled with the high reaction rates at 600°C, makes the total impedance of the electrical double layer resistance-limited rather than capacitance-limited.

The combination of a non-reproducible unsteady (several millivolts) equilibrium potential and the very low resistance of the electrical double layer makes determination of active surface area by the coulostatic method very unreliable. Molten-carbonate fuel cells probably will not be investigated further by this method.

C. Task I-1b. Study Effects of Varying Electrode Fabrication Techniques

Variables to be investigated in this task include:

(1) particle size of starting materials
(2) pressing pressure, time and temperature
(3) sintering time, temperature and atmospheres
(4) binders, burnout and leachable additives.

Fabrication techniques for porous electrode structures are concentrated on the use of silver, stainless steel, nickel and nickel alloys, including stellite alloys (Ni, Cr, CrB). Studies are being made on the effects of particle size, size range, pressure, sintering temperature, sintering time, and the use of binders on the pore structure and strength of the electrode structure.

It has been established, particularly in the fabrication of silver electrodes, that compacting pressures are quite critical. The silver particles are very ductile. Even under 1000 psi pressure, they are compacted to such a degree that very little porosity remains. An electrode with uniform porosity and sufficient strength can be fabricated by heating loosely packed 100-200 mesh silver powders to 850°C under a pressure of approximately 1 psi.

Suitable nickel and Raney nickel electrode structures have not yet been fabricated. However, strong structures have been achieved with 200 mesh stellite powders using a carbowax binder and pressing at 60,000 psi. These compacts are sintered at 950°C in an atmosphere of H_2 for 1-2 hours and cooled in an atmosphere of helium. This work is continuing.

D. Task I-1c. Study Effects of Electrode and Electrolyte Composition

The effect of varying the composition of the electrolyte on cell performance was studied by adding other salts to the binary $LiNaCO_3$ eutectic.

Six experimental fuel cells were run with similar fuel and air electrodes and various salts added to the electrolyte. Performance characteristics are tabulated on the following page.

The fuel electrode consisted of 5.0 gms of a mixture of 60% carbonyl nickel, 30% silver (-325 mesh), and 10% zinc (-325 mesh) blended with 20% carbonate burn-out material (50-150 mesh) and sintered at 800°C. The air electrode was made of silver, 3 gms of 80-100 mesh and 3 gms 100-150 mesh, sintered at 850°C. Electrode area was 1/60 sq ft.

Cell #	Additive	Mole %	Peak Pwr	Activation Time to Peak Pwr	Operating Temp.
132	Blank	-	48.8 wsf	8 hours	600°C
133	Na_2MoO_4	8.6	48.3	1 day	600°C
134	Na_2CrO_4	8.6	32.3	2 days	600°C
135	Na_2WO_4	10.0	42.0	2 hours[1]	600°C
136	Na_2S	10.0	61.7	1 day	600°C
137	Na_2ZnO_2	5.0	42.8	2.5 hours[2]	600°C

[1]Rapid performance deterioration in 24 hours

[2]Rapid performance deterioration in 48 hours

In cells #135 and 137, the internal resistance rose abnormally (Fig. 12) after only a few days of operation. This effect probably resulted from precipitation of the additives Na_2WO_4 and Na_2ZnO_2 in the pores of the MgO matrix.

The fuel electrodes used in this series of experiments have typically shown slow activation, higher internal resistances, and only moderate power levels (40-50 wsf). Lifetimes have generally been less than 30 days. Catalyst-impregnated silver electrodes are capable of better performance.

All the additives, with the exception of Na_2WO_4 and Na_2CrO_4, seemed to lower the internal resistance initially (Fig. 12) from that normally observed during the first few days of operation of this type of fuel electrode with pure binary carbonate electrolyte.

This effect may be attributed to a faster reduction of NiO in the fuel electrode by the hydrogen under the influence of the additive. Possibly H_2 is more soluble in the mixed melt or the NiO film may be more pervious in the presence of these oxy-anions.

After only a few days operation (only 1 day in the case of Na_2ZnO_2), the internal resistance of the cells started to rise markedly and power output

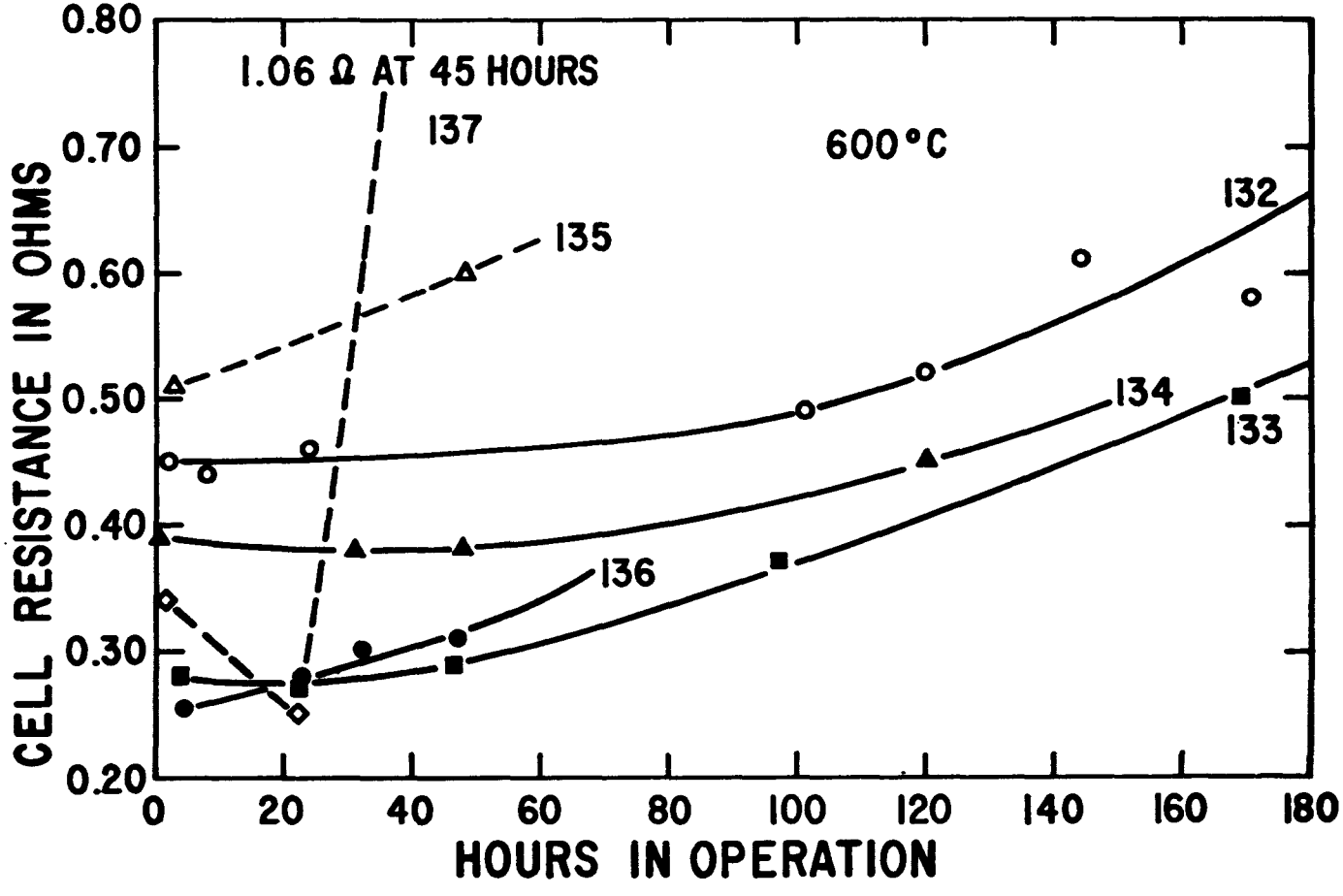

Fig. 12 Cell Resistances with Different Electrolyte Additives

fell. This effect may be caused by decomposition of the electrolyte and/or additive with a resulting increase in Na_2O content and corresponding drop in mobility of ions in the melt.

In this series of cells, a relatively poor fuel electrode which is known to be subject to flooding problems was used, because it was thought any significant change of wetting characteristics or oxide ion concentration would be dramatically illustrated. Only Na_2S addition resulted in marked improvement in power output. This effect is now thought to have been caused by an attack by the $S^=$ on the Ag of the air electrode, with a resulting increase in surface area and a decrease in polarization. This solution of Ag eventually can lead to Ag dendrite shorts through the MgO disc.

This series of experiments confirms the supposition that electrolyte conductivity and wetting in the MgO matrix cell are not limiting cell performance now. Until these properties can be shown to limit cell power output, additional experiments should be suspended.

We have performed a number of experiments varying the composition of the fuel (anode) electrode. The tests were carried out in operating cells, with particular emphasis on power output and lifetime. The following electrodes have been recommended for use in development of the prototype systems:

Anode - silver matrix, dual porosity, 100-120 mesh and 120-150 mesh, impregnated with NiO,

Cathode - silver matrix, dual porosity, 80-100 mesh, 100-150 mesh.

Other factors considered in selecting these electrodes included ease of preparation and reproducibility.

E. Task I-2, Electrode Fabrication

Further consideration of the variations of electrode configuration as planned for this task has indicated that little work is justified. The

cylindrical electrode has been found to have a basic limitation in the ability to attain high power output per unit volume; there seem to be no strong offsetting arguments. The cell modules under development will be operated horizontally, primarily to demonstrate the system's degree of tolerance to orientation variation.

The effort planned for this area will be placed instead on the development of the partial oxidation process for handling JP-4 jet fuel.

F. Task I-3. Battery Assembly

By J. K. Truitt, B. H. Barbee, T. N. Hooper, and A. H. White

1. Introduction

With the development of molten-carbonate research cells as a basis, a larger integrated system designed to produce 100 watts is to be developed. This section of the study is in three parts as follows:

(a) Assemble cells to produce 100-watt batteries and test their mechanical and electrochemical characteristics.

(b) Study effects on cell performance and life of quick start-up times and cycling of the cells (from 30°F to operating temperature).

(c) Deliver a portable battery system of 100 watts that will have its own self-contained heater, fuel supply, and carbon-dioxide recirculating mechanism.

All emphasis during the first quarter has been on items (a) and (c). The cycling and start-up studies will be carried out when the 100-watt battery has been developed. We now plan to raise to 400 watts the output of the demonstration model to be delivered.

2. Task I-3a.

Single cell units that closely approximate battery conditions have been used to further reliability, materials, and systems engineering.

Known variables must be held constant while new variables are imposed upon the cell. Several new variables were examined.

Our supplier of MgO discs sent two of a new type for evaluation. The regular type, LM 833, has 31% porosity and 18 micron pores, while the two new ones, LM 833A, have 40% porosity and 24 micron pores. Cells #410 and 411 were made with this new variable. Figures 13 through 18 represent the data under various operating conditions. All cells are brought up to temperature with small flows of H_2 at the anode and CO_2 at the cathode. Operating time is started when air is introduced to the cathode. Figures 13 and 17 show the rapid activation when air is added. Actually, the response is essentially instantaneous to about 75% of maximum power obtained after 8-10 hours.

For a more efficient fuel utilization, series fuel flow is incorporated in the battery configuration. Reaction products are CO_2 and H_2O, which dilute the fuel to downstream cells. A synthetic mixture was made to approximate the fuel as seen by the last cell in a 100-watt battery module. Figures 14, 15 and 16 represent these data. The considerable power loss emphasizes the need to consider these realistic fuels rather than H_2 in our studies.

Cell resistance from electrodes to load has drawn considerable attention during this report period. The difference between the two curves in Fig. 18 is represented only by lead wire resistance from furnace to X-Y recorder. This represents a 12% increase in power and places us at a stated objective of 100 watts/ft^2 at 0.7 volts on hydrogen fuel. Further modifications of electrical leads should result in increased power. Cell #414 was built with our regular disc for comparison with the new type disc. Figures 19 and 20 show similar performance.

A post-mortem examination of cell #410 (LM 833A disc) revealed a laminar disc structure that gave way to the thermal stresses of the electrodes and consequently, a separation and increased resistance. The other new disc

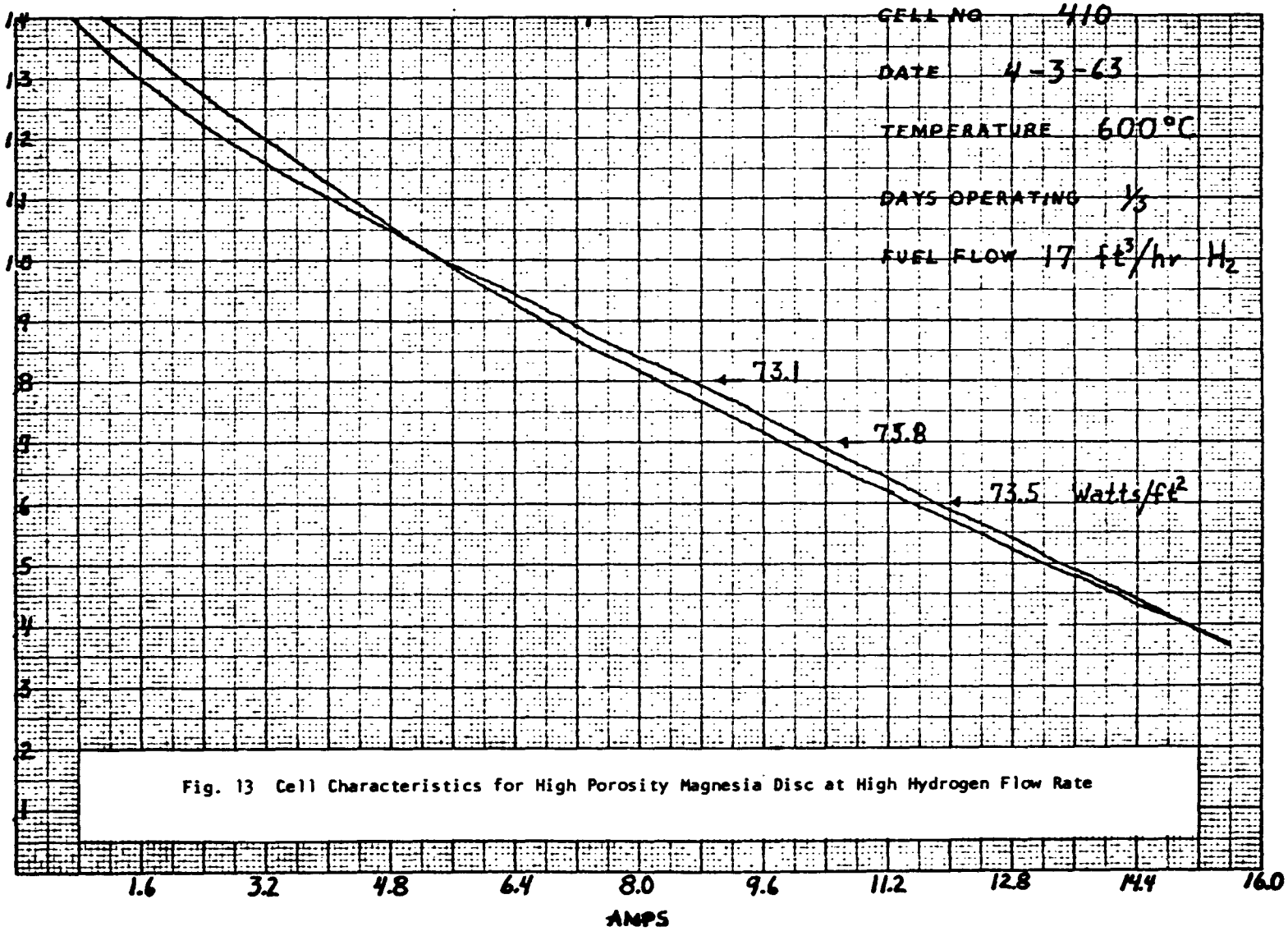

Fig. 13 Cell Characteristics for High Porosity Magnesia Disc at High Hydrogen Flow Rate

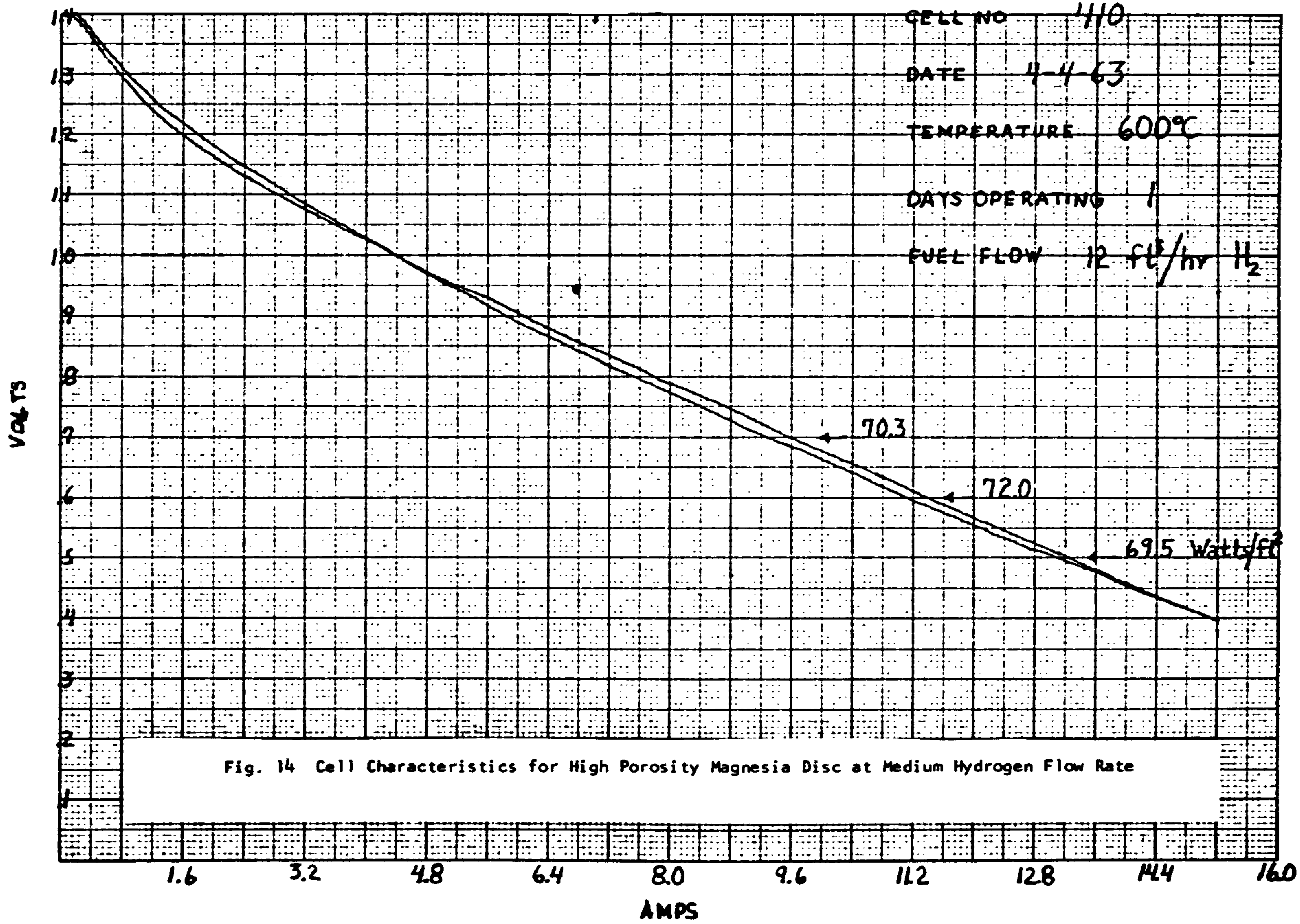

Fig. 14 Cell Characteristics for High Porosity Magnesia Disc at Medium Hydrogen Flow Rate

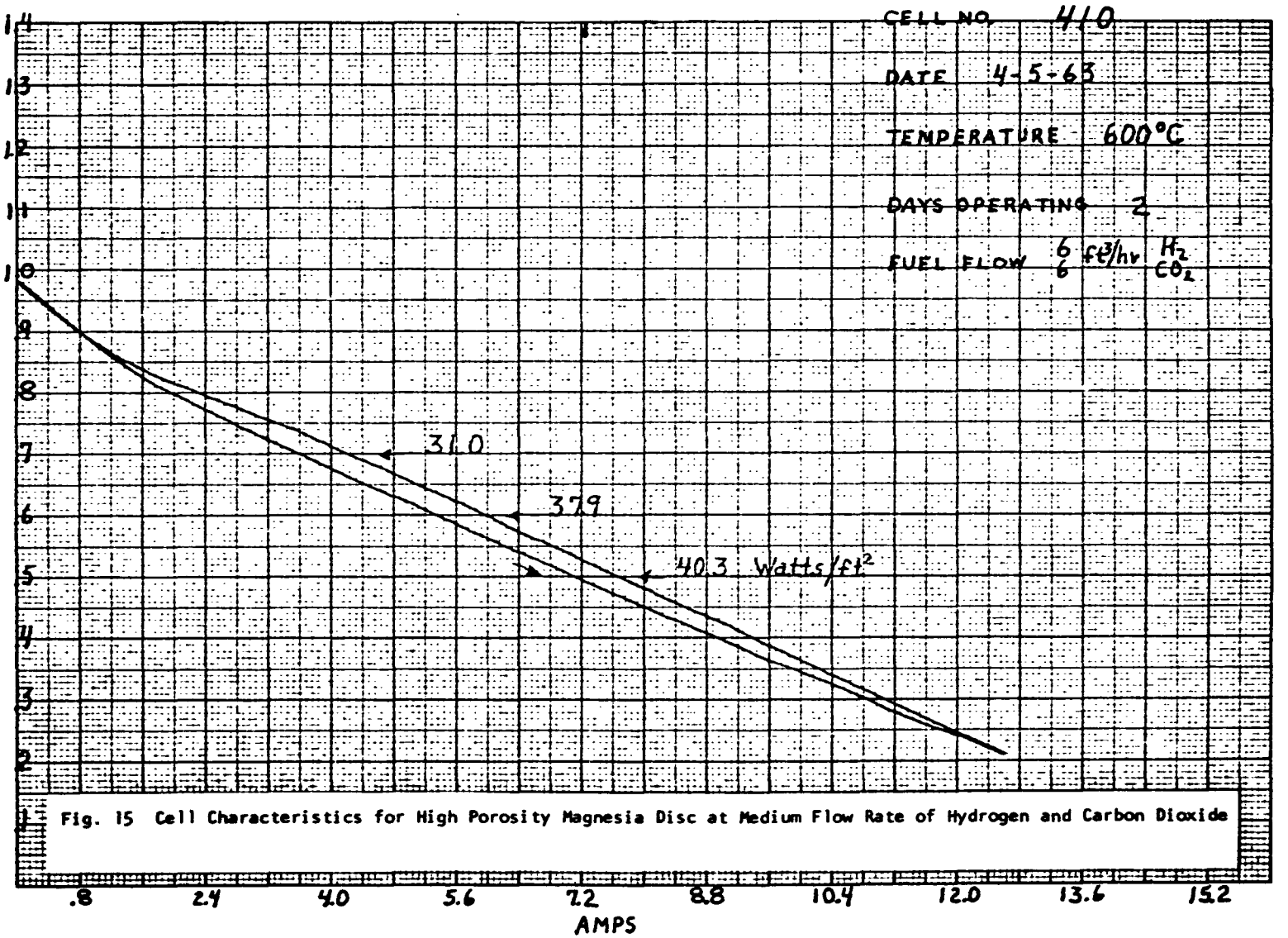

Fig. 15 Cell Characteristics for High Porosity Magnesia Disc at Medium Flow Rate of Hydrogen and Carbon Dioxide

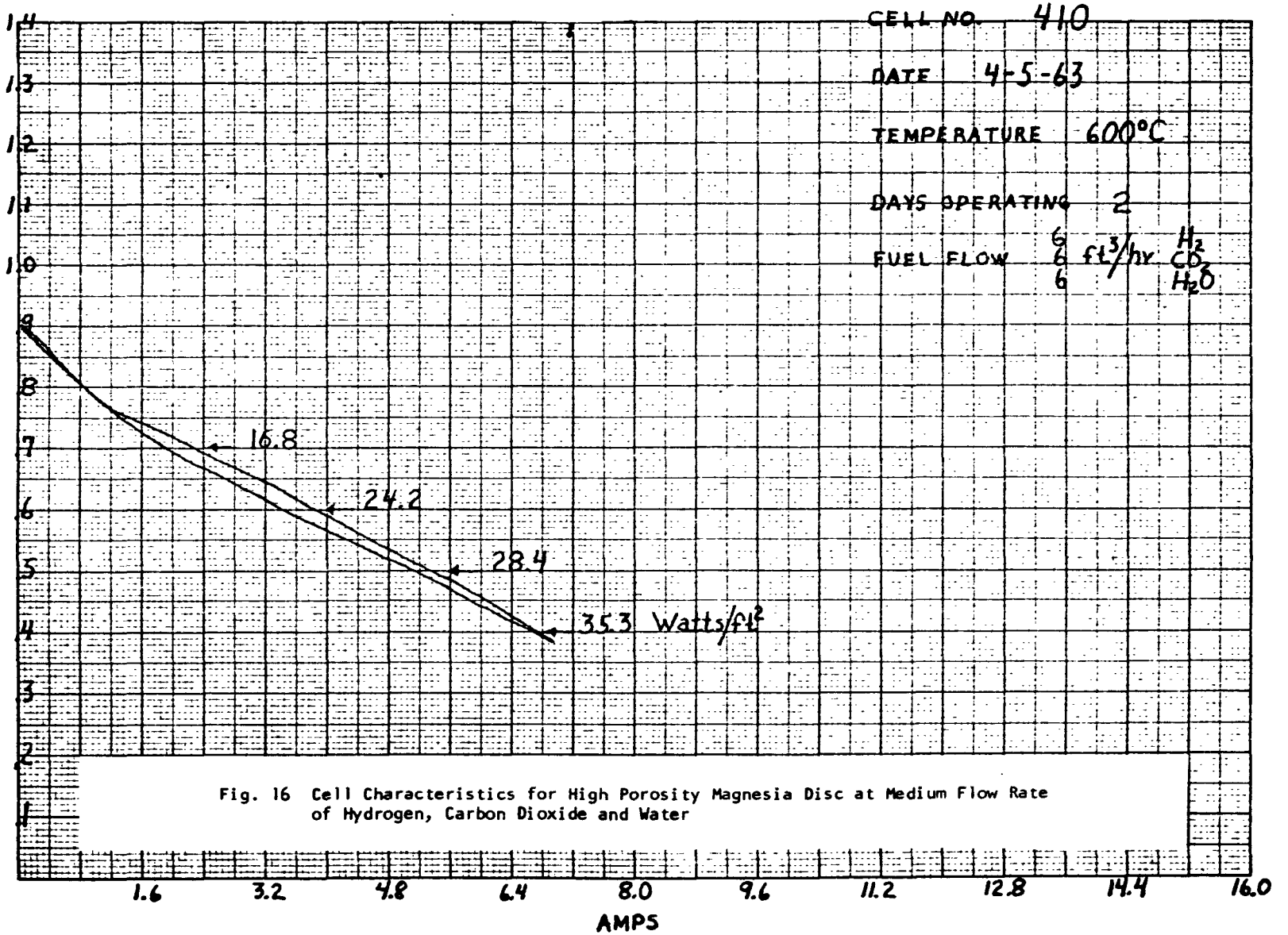

Fig. 16 Cell Characteristics for High Porosity Magnesia Disc at Medium Flow Rate of Hydrogen, Carbon Dioxide and Water

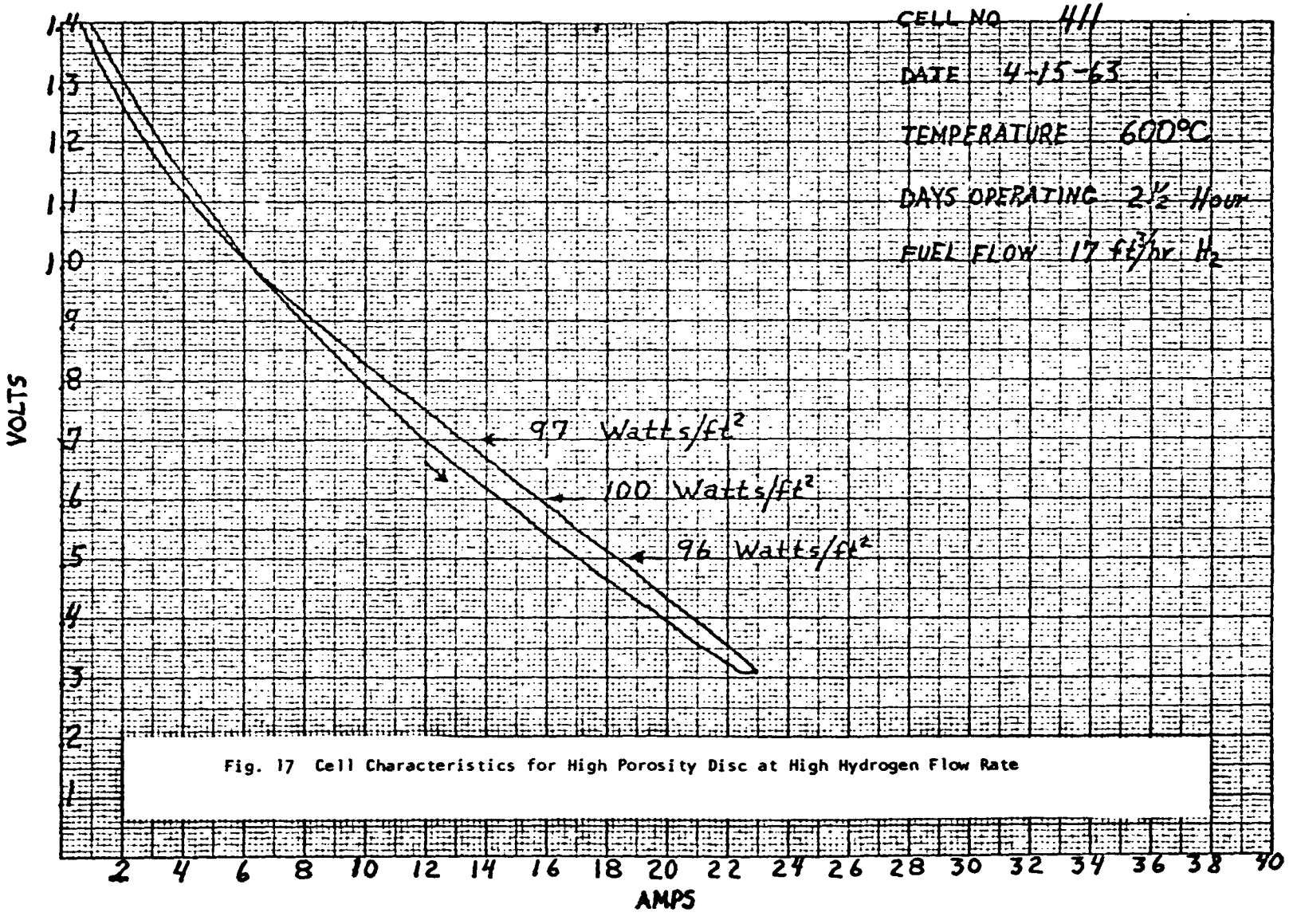

Fig. 17 Cell Characteristics for High Porosity Disc at High Hydrogen Flow Rate

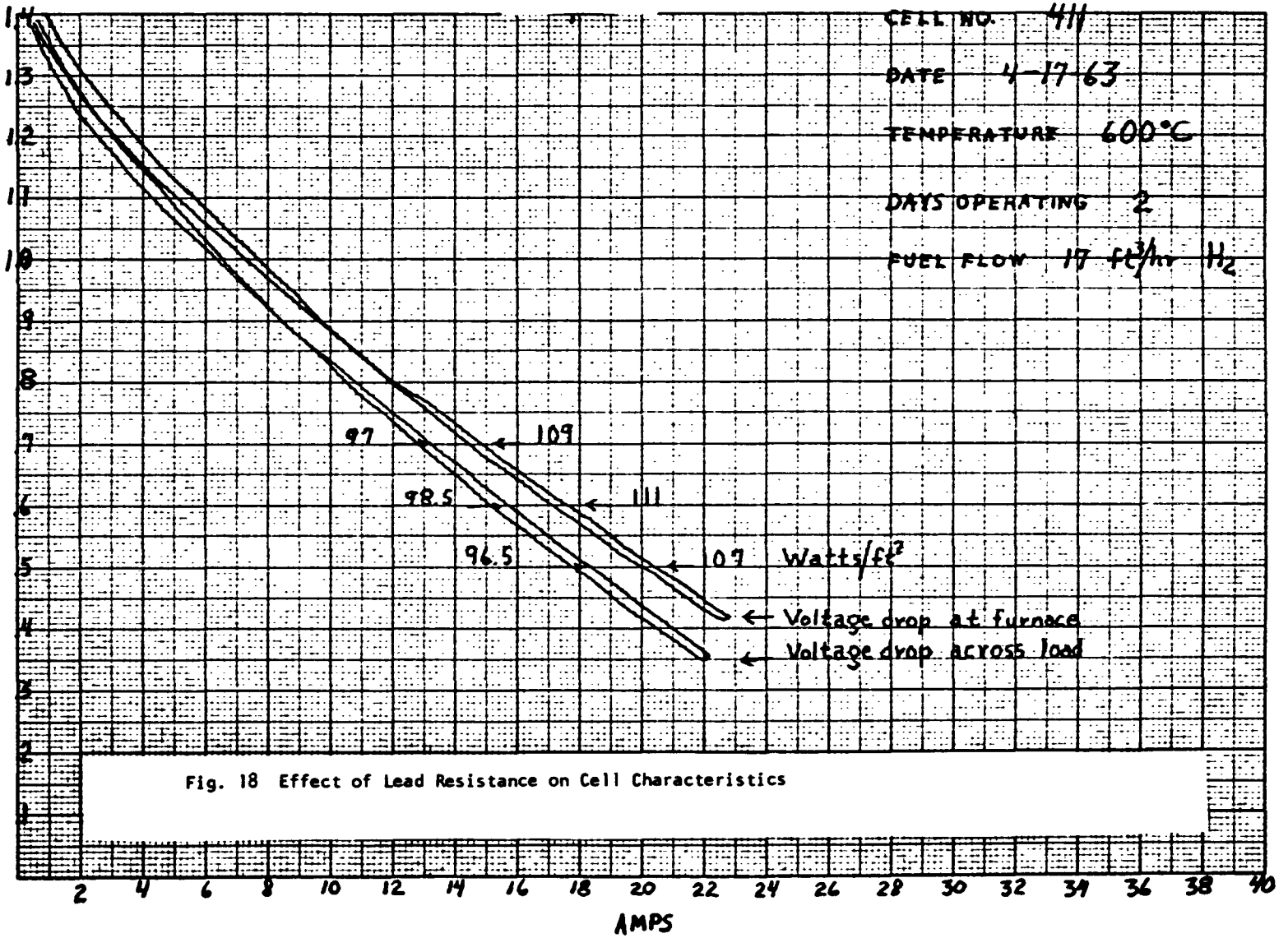

Fig. 18 Effect of Lead Resistance on Cell Characteristics

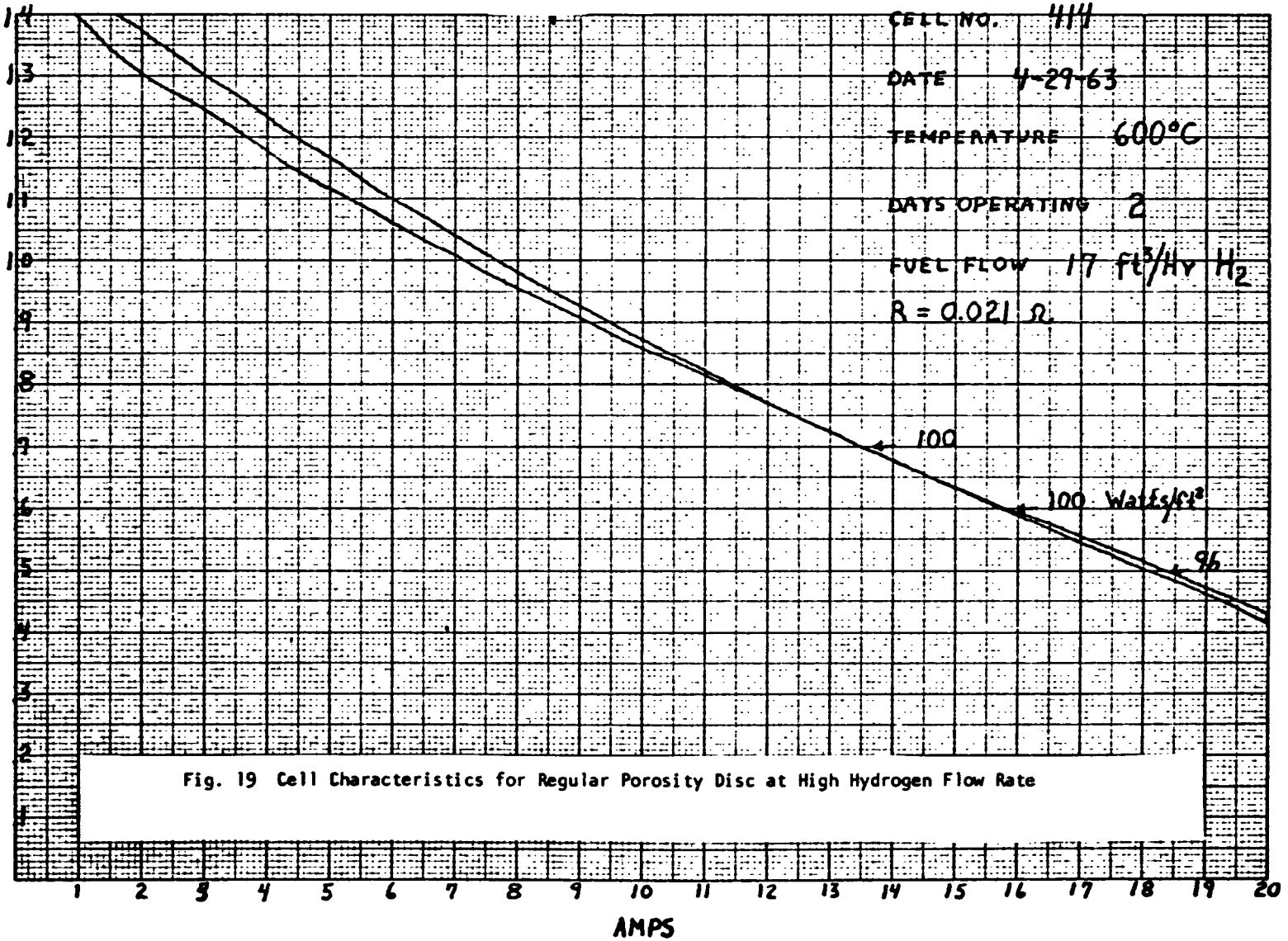

Fig. 19 Cell Characteristics for Regular Porosity Disc at High Hydrogen Flow Rate

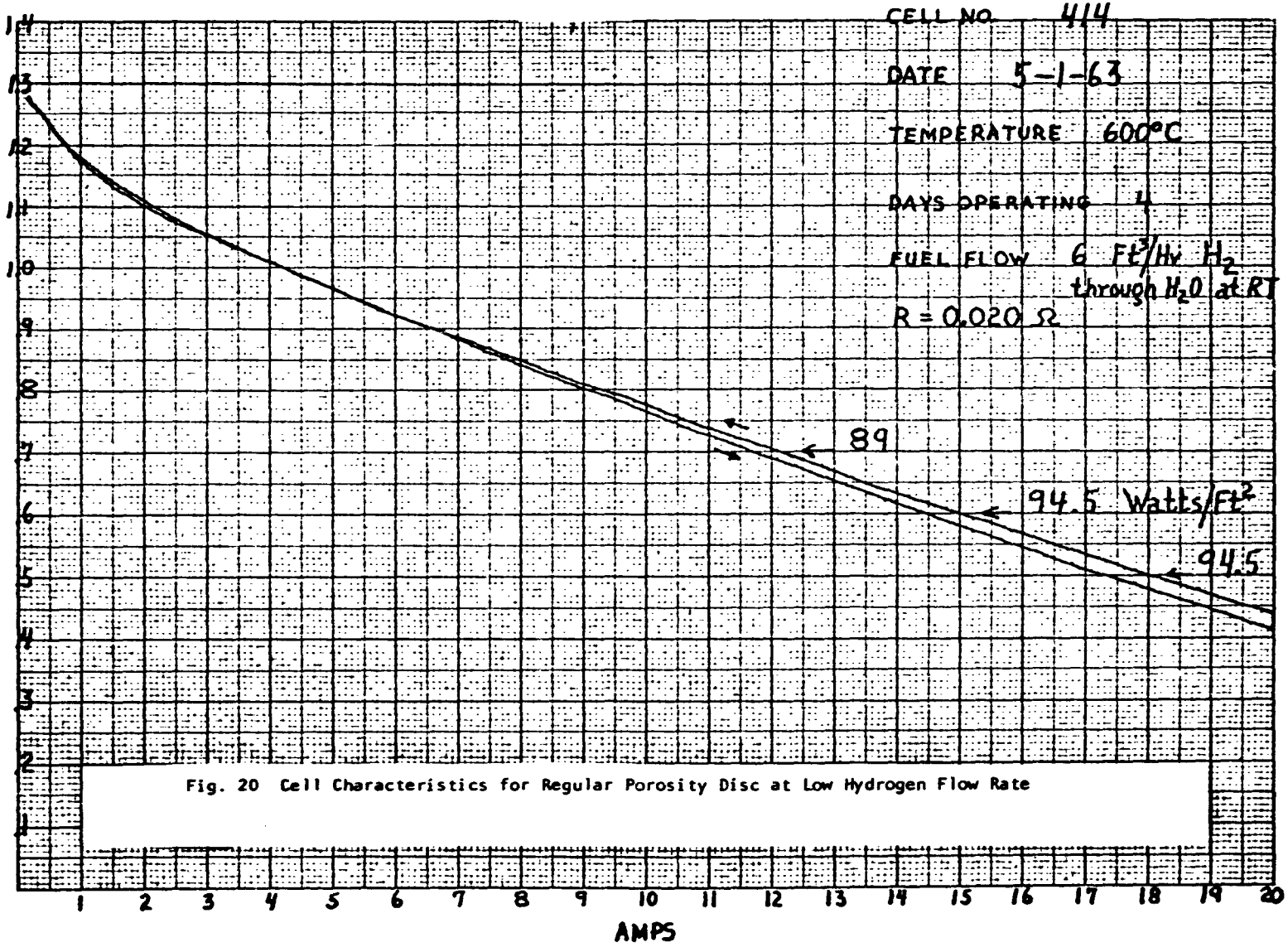

Fig. 20 Cell Characteristics for Regular Porosity Disc at Low Hydrogen Flow Rate

does not show this laminar structure, but a complete examination has not yet been made. The supplier will send additional discs for further evaluation.

Work on the development of the 100-watt battery is progressing. A unit is shown in Figs. 21 and 22. Figure 21 shows the internal structure and Fig. 22, the complete battery module. The battery module consists of a number of steel rings. Two MgO discs are sealed to the metal ring in a manner to permit gas passage between like electrodes. (See Fig. 23.) Likewise, adjacent rings packaged within a sheet metal cylinder form a gas passage. The gas passages formed inside the rings are connected via metal tubes. The gas passages between the rings are connected via 7 holes completely through the ring. Thus, we have a series gas flow for utilizing fuel. The electrodes in a cell are connected in parallel to avoid the need for many expensive components such as bi-polar plates, electrical feedthroughs, and individual electrolyte supply. The over-all result is as if one took a very large MgO plate with electrodes and folded it "accordion fashion" into a compact package.

For the battery, we have chosen a basic cell package of 1.3 sq ft of electrode surface, which is achieved by mounting 14 discs in 7 rings. This cell package is connected in series to a similar package to form the modular battery. This is accomplished by simply taking a package of 14 discs with air electrodes shorted to the rings (ground) and attaching it to a package with fuel electrodes grounded. Thus, the battery is basically two cells in series.

Test cells containing a single MgO disc and electrodes as described above have produced 100 watts/ft^2 when provided a good sweep of H_2. Therefore, one might assume that a module with 2.6 sq ft of electrode surface would produce 260 watts. However, when one considers that the ERDL battery will operate on a hydrocarbon fuel and that a series flow of gas will deliver a further diluted fuel to the downstream electrodes, the factor of safety provided in TI's module appears reasonable.

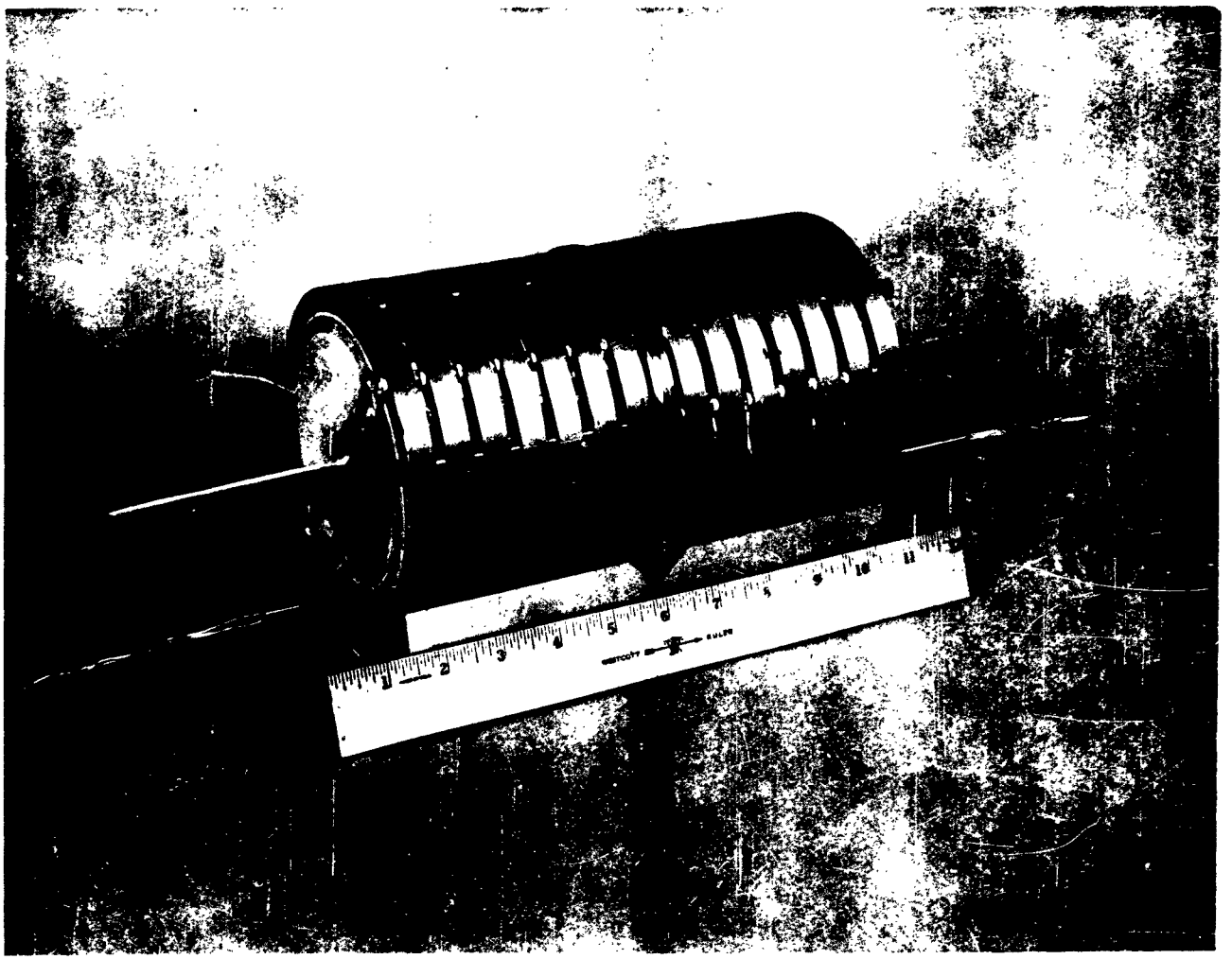

Fig. 21 Interior of Modular Battery

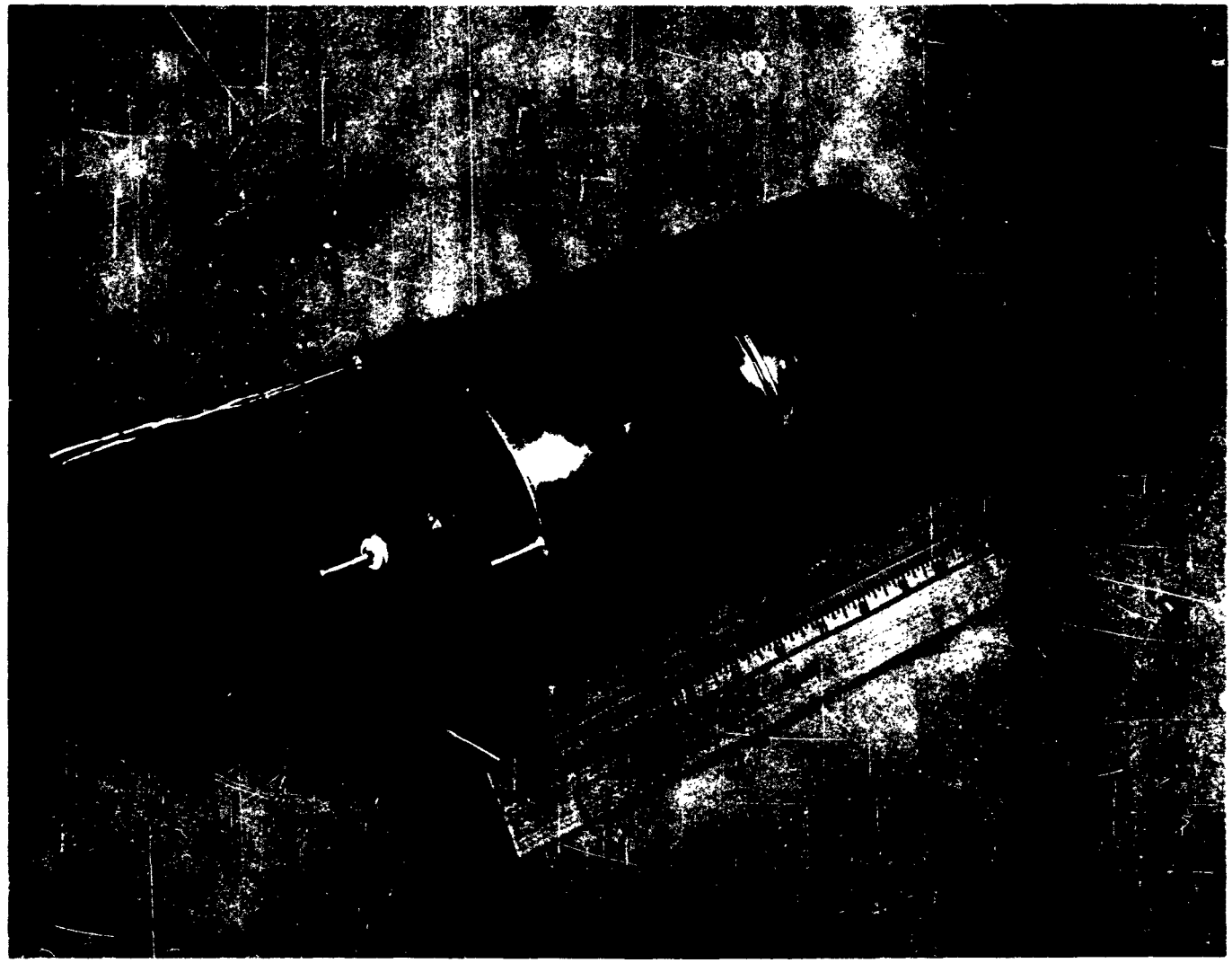

Fig. 22 Complete Modular Battery

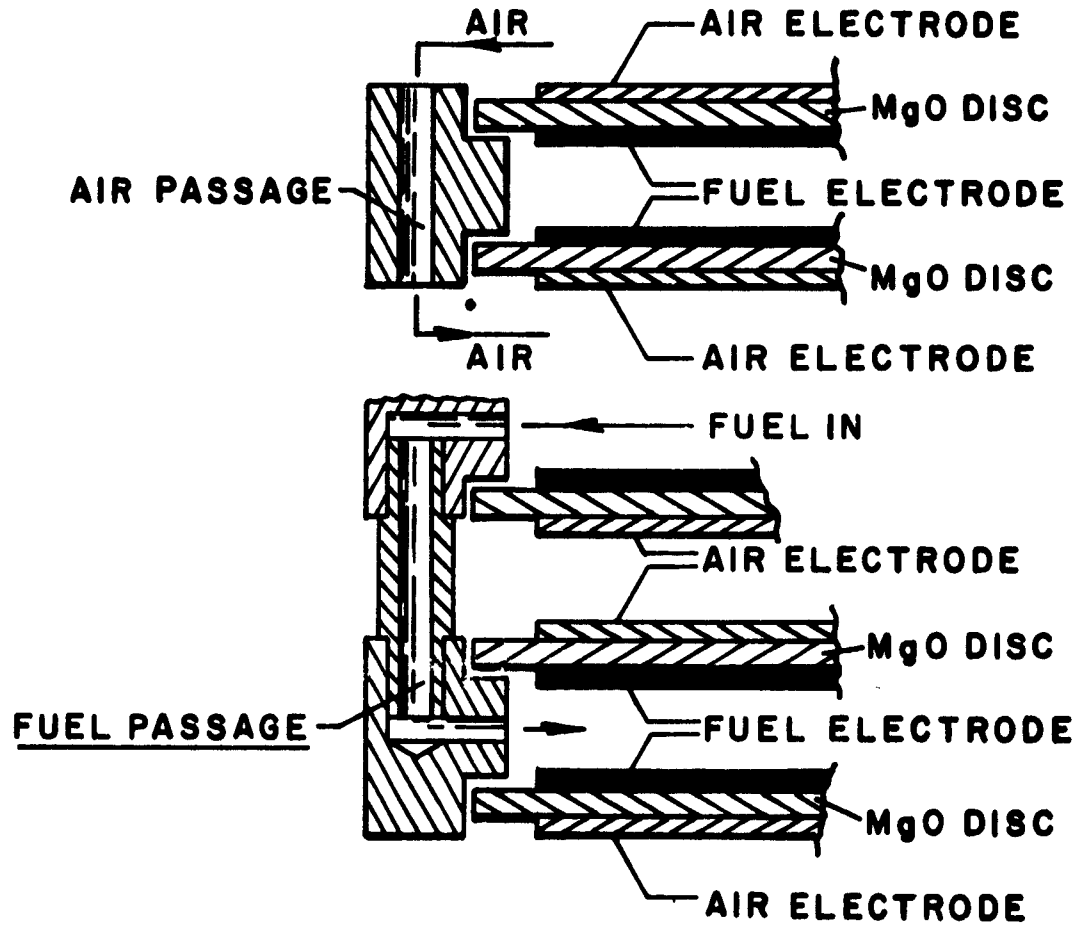

Fig. 23 Flow Pattern for Modular Battery

Three test modules have been assembled to date. The first developed internal shorting; the second had a structural defect causing a restriction of gas flow. The third has just been placed in operation and appears to be performing properly. Performance will be summarized in a later report.

3. Task I-3c. Self-Contained Fuel Supply

a. Laboratory Tests

Satisfactory yields of hydrogen have been obtained from a bench-scale partial oxidation process and were concluded with a 78-hour optimization run. Best results were obtained near the end of this run and are indicated by the following chromatographic analysis.

Component in Dry Gas Sample	% Vol.
H_2	36.0
N_2	31.8
CO	25.2
CH_4	3.0
C_2H_6	--
CO_2	4.0
C_2H_4	--

Design and operation of this process was based on the following chemical reactions utilizing jet fuel, Grade JP-4 (MIL-J-5624E).

(1) 70% air partial oxidation:

$$0.7(CH_2)_{10} + 2.5\ O_2 + 14N_2 \rightarrow 7.0\ CO + 14\ N_2 + 7\ H_2$$

ΔH = - 160,000 BTU/lb Mole

(2) 30% Non-catalytic steam reforming:

$$0.3(CH_2)_{10} + 3\ H_2O \rightarrow 3.0\ CO + 6\ H_2$$

ΔH = + 251,000 BTU/lb Mole

(3) 100% Shift conversion:

$$10\ CO + 10\ H_2O \rightarrow 10\ CO_2 + 10\ H_2$$

ΔH = + 37,000 BTU/lb Mole

Combined reaction:

$$1.0\ (CH_2)_{10} + 3.5\ O_2 + 14\ N_2 + 13\ H_2O \rightarrow 14N_2 + 10\ CO_2 + 23\ H_2$$
$$\Delta H = +\ 128{,}000\ \text{BTU/lb Mole}$$

The combined equation represents partial oxidation of the hydrocarbon; 70% of the oxygen required for partial combustion is supplied by air and the remaining 30% oxygen plus additional oxygen to convert CO to CO_2 comes from steam. In addition, water used in the reaction helps lessen the tendency toward coke formation through disproportionation of CO. The "70% partial air oxidation" is further based on nearly balanced thermal requirements at 2200°F for exothermic partial oxidation and endothermic noncatalytic reforming of the remaining 30% of hydrocarbon. By balancing thermal requirements and operating at relatively low temperature, we have been able thus far to use metal pipe as a tubular reactor, thereby eliminating the need for high temperature refractory-lining in the reactor. Although the heat load is almost balanced, a zone-type reaction is probably carried out and heat is supplied to the reactor to make up heat losses from the overall reaction.

A reliability test fuel cell was operated directly off the partial oxidation product stream, with approximately 65% reduction in power output at 0.7 volts compared to performance on pure hydrogen. Figure 24 shows a comparison of performance. During this operation, H_2 and CO concentrations in the dry gas partial oxidation product were 26.2 - 41.0% V and 17.2 - 30.6% V respectively. With the setup illustrated in Fig. 25, we used the following procedure to conduct the laboratory experiments.

(1) Air, water and JP-4 fuel (ca. $C_{10}H_{20}$) were metered, line-mixed and preheated in a tubular coil to 500°F.

(2) The totally vaporized and mixed feed stream at ca. 25 psig was then injected to the tubular metal reactor through a variable orifice nozzle. Reaction temperature was usually maintained at 2200°F, although operation at 2000°F also produced good results.

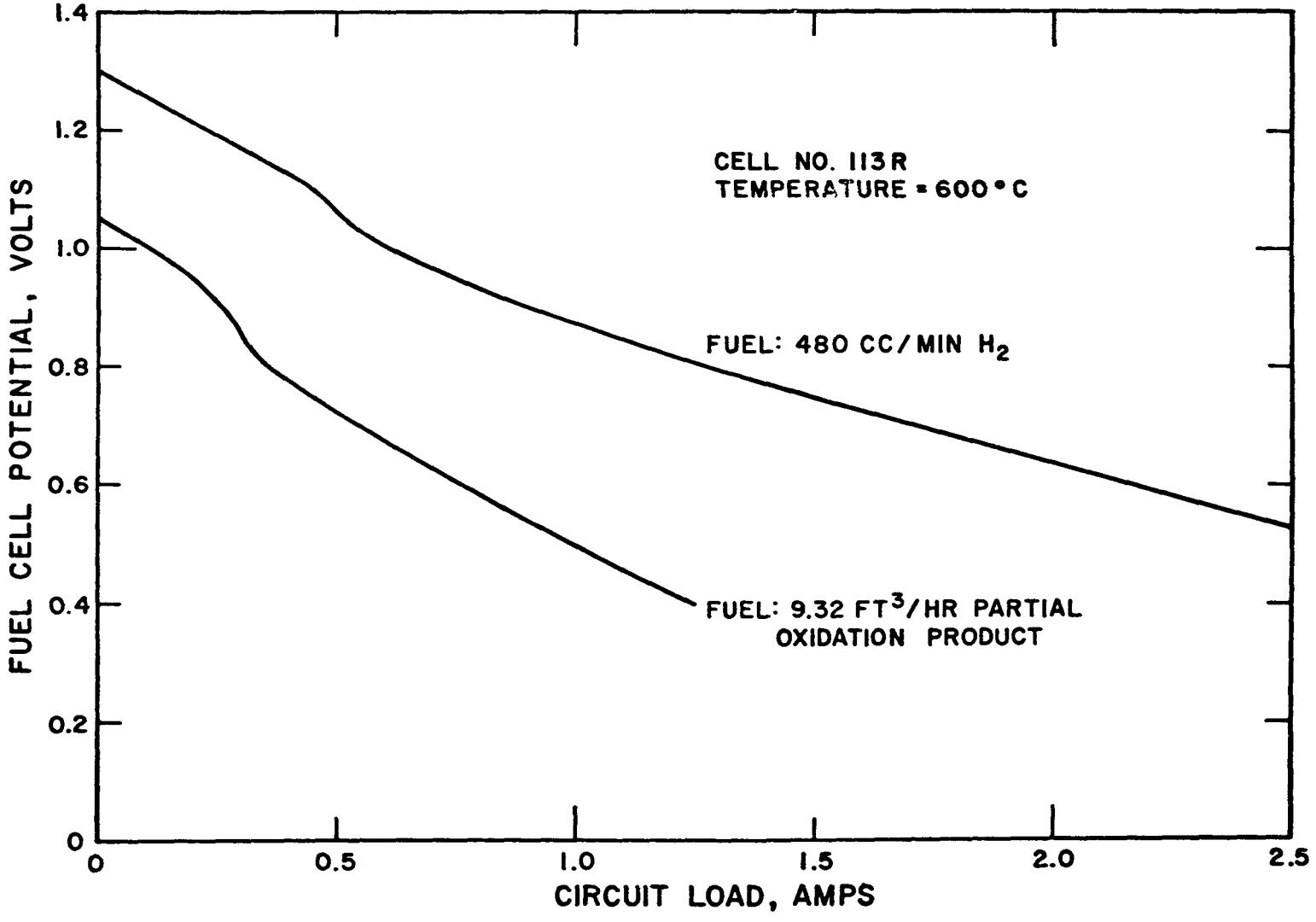

Fig. 24 Comparison of Cell Performance - Hydrogen vs Partially Oxidized JP-4 Jet Fuel

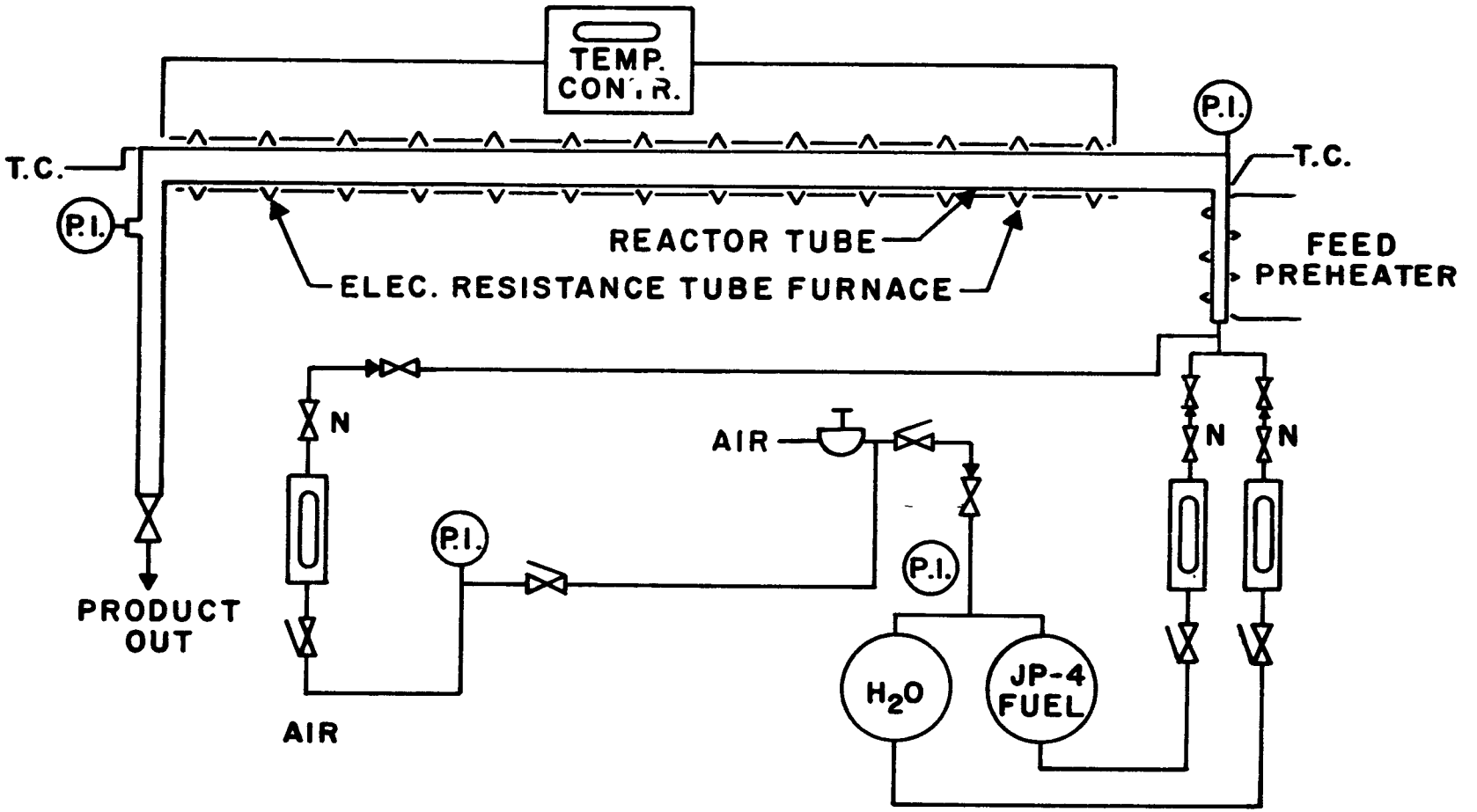

Fig. 25 Laboratory Setup for Evaluation of Partial Oxidation Process

(3) The reaction product (9.32 cfh) at ca. 0 psig was then fed directly to the molten-carbonate fuel cell at 600°C through an insulated line; cell operation on an integrated fuel supply was thereby accomplished.

Figure 26 shows the variation of product gas composition during the previously mentioned 78-hour optimization run as revealed by periodic chromatographic analyses. Relatively close monitoring of the system was necessary because flow metering was not pressure-compensated. This is illustrated by the wide swings in composition experienced after 28 1/2 hours operation, when the process was run unattended.

b. Pilot Plant Studies

Design of a 50-70 cfh 70% partial oxidation process is approximately 100% complete. Mechanical design of a pilot plant is approximately 80% complete; fabrication has started and is approximately 10% complete. We plan to use this unit as a fuel source in the 400-watt fuel cell demonstration unit. The flow sheet (Fig. 27) illustrates the proposed incorporation of the partial oxidation unit.

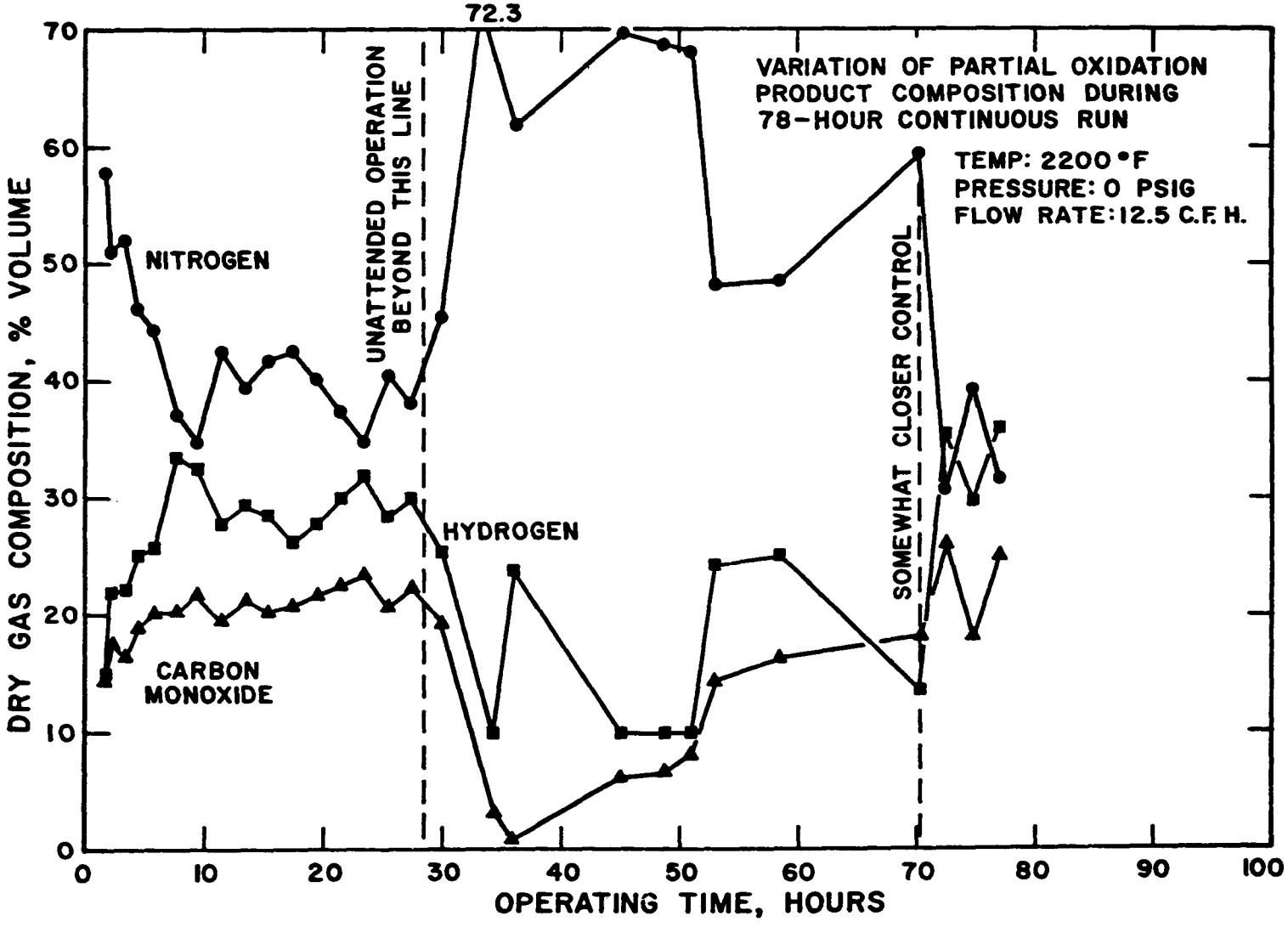

Fig. 26 Laboratory Partial Oxidation Unit Performance

50 C.F.H. 70% PARTIAL OXIDATION PROCESS WITH TWO-STAGE FUEL INJECTION

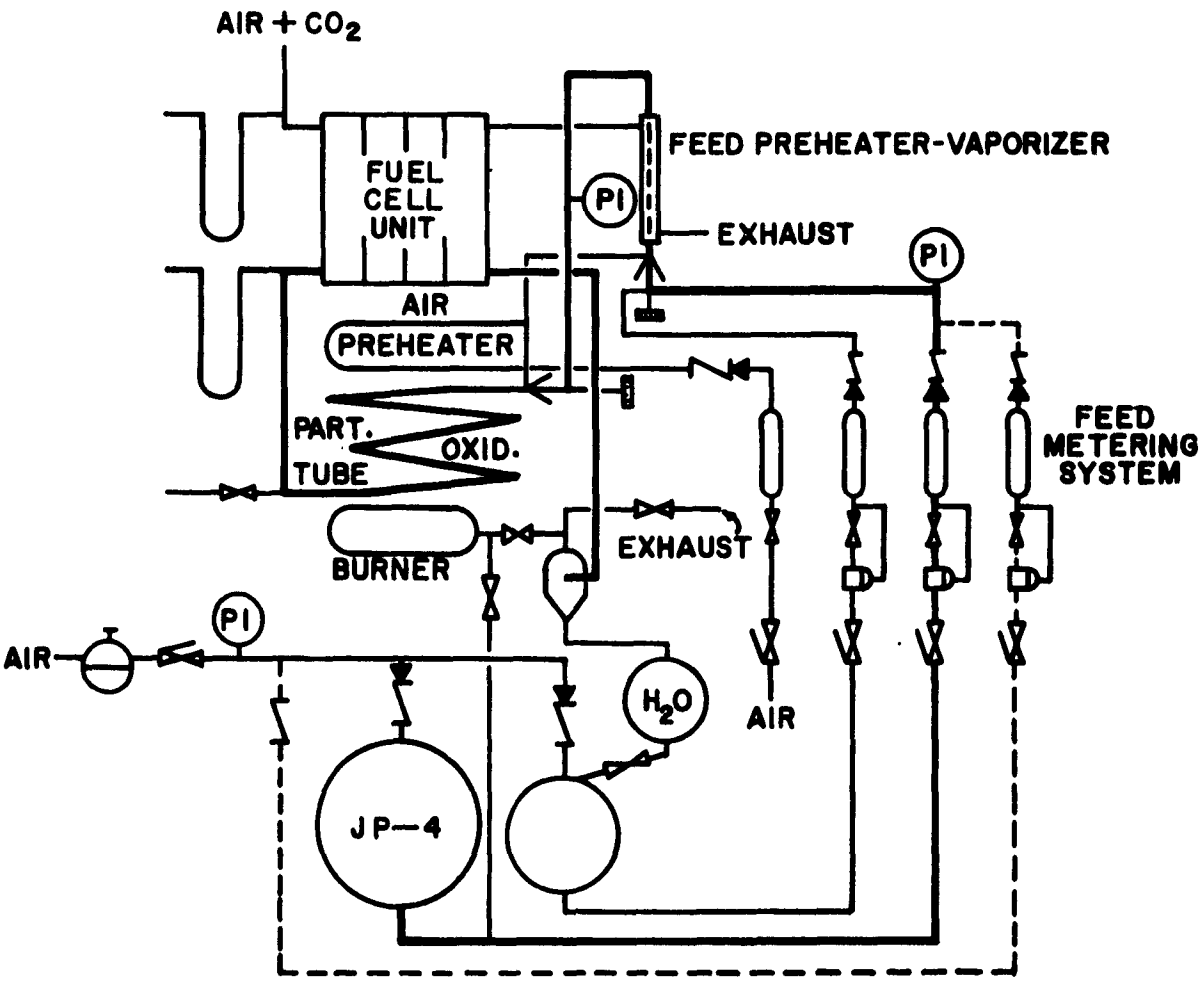

Fig. 27 Design of 50 CFH Partial Oxidation Unit

III. CONCLUSIONS

(1) Cell performance has been improved by control of electrode structure, reduction of resistance and improved gas flow. Outputs of 100 watts/ft^2 have been attained on pure hydrogen.

(2) A battery module has been constructed, and indications are that it will operate satisfactorily. However, some design changes and improvements are indicated.

(3) Partial oxidation with air has been demonstrated as an effective process for converting JP-4 to a suitable fuel for the molten-carbonate fuel cell.

IV. PLANNED WORK

(1) Continue studies leading to improved power output through reduction in cell polarization.

(2) Study durability of a number of metals and ceramics in environmental conditions of cell.

(3) Continue development of the battery module for reliability.

(4) Complete and test the 50-70 cfh partial oxidation unit and run preliminary combined tests with the battery module.